This article is a *Plant Cell* Advance Online Publication. The date of its first appearance online is the official date of publication. The article has been edited and the authors have corrected proofs, but minor changes could be made before the final version is published. Posting this version online reduces the time to publication by several weeks.

Sufficient Amounts of Functional HOP2/MND1 Complex Promote Interhomolog DNA Repair but Are Dispensable for Intersister DNA Repair during Meiosis in *Arabidopsis*[W]

Clemens Uanschou,[a,1] Arnaud Ronceret,[b,c,1,2] Mona Von Harder,[a,1] Arnaud De Muyt,[b,c,3] Daniel Vezon,[b,c] Lucie Pereira,[b,c] Liudmila Chelysheva,[b,c] Wataru Kobayashi,[d] Hitoshi Kurumizaka,[d] Peter Schlögelhofer,[a,4] and Mathilde Grelon[b,c]

[a] Department of Chromosome Biology, Max F. Perutz Laboratories, University of Vienna, A-1030 Vienna, Austria
[b] Institut National de la Recherche Agronomique, Unité Mixte de Recherche 1318, Institut Jean-Pierre Bourgin, F-78000 Versailles, France
[c] AgroParisTech, Institut Jean-Pierre Bourgin, F-78000 Versailles, France
[d] Graduate School of Advanced Science and Engineering, Waseda University, Shinjuku-ku, Tokyo 162-8480, Japan

During meiosis, homologous recombination (HR) is essential to repair programmed DNA double-strand breaks (DSBs), and a dedicated protein machinery ensures that the homologous chromosome is favored over the nearby sister chromatid as a repair template. The HOMOLOGOUS-PAIRING PROTEIN2/MEIOTIC NUCLEAR DIVISION PROTEIN1 (HOP2/MND1) protein complex has been identified as a crucial factor of meiotic HR in *Arabidopsis thaliana*, since loss of either MND1 or HOP2 results in failure of DNA repair. We isolated two mutant alleles of *HOP2* (*hop2-2* and *hop2-3*) that retained the capacity to repair meiotic DSBs via the sister chromatid but failed to use the homologous chromosome. We show that in these alleles, the recombinases RADIATION SENSITIVE51 (RAD51) and DISRUPTED MEIOTIC cDNA1 (DMC1) are loaded, but only the intersister DNA repair pathway is activated. The *hop2-2* phenotype is correlated with a decrease in HOP2/MND1 complex abundance. In *hop2-3*, a truncated HOP2 protein is produced that retains its ability to bind to DMC1 and DNA but forms less stable complexes with MND1 and fails to efficiently stimulate DMC1-driven D-loop formation. Genetic analyses demonstrated that in the absence of DMC1, HOP2/MND1 is dispensable for RAD51-mediated intersister DNA repair, while in the presence of DMC1, a minimal amount of functional HOP2/MND1 is essential to drive intersister DNA repair.

INTRODUCTION

A specialized type of cell division, called meiosis, ensures the reduction of the genome prior to the formation of generative cells. During meiosis, genetic information between maternal and paternal chromosomes is exchanged, leading to novel combinations of genetic traits in the following generation. The molecular basis of this process is recombination between homologous chromosomes. Meiotic homologous recombination is initiated with the programmed induction of DNA double-strand breaks (DSBs) induced by the conserved Sporulation11 (Spo11) protein (Bergerat et al., 1997; Keeney et al., 1997; Malik et al., 2007). Following meiotic DSB formation, Spo11 is removed from the DNA by a single-stranded DNA (ssDNA) nick next to the DSB site (Keeney and Kleckner, 1995; Neale et al., 2005; Garcia et al., 2011; Pan et al., 2011). Subsequent nucleolytic resection yields 3′-primed, single-stranded DNA, which serves as a probe for finding a repair template. The ssDNA strand is associated with protein factors to form a nucleoprotein filament that then mediates strand invasion (single end invasion) into an intact DNA duplex (reviewed in Pâques and Haber, 1999; reported in Hunter and Kleckner, 2001; Neale and Keeney, 2006; Edlinger and Schlögelhofer, 2011).

In a diploid cell, after replication, the DNA template for repair can either be one of the two chromatids of the homolog or sister chromatid. During meiosis, only a selected number of Spo11-catalyzed DSBs proceed to form crossovers (COs; reciprocal exchange between chromosomes) (Schwacha and Kleckner, 1994, 1997; Allers and Lichten, 2001; Hunter and Kleckner, 2001). These ensure subsequent regular chromosome disjunction at meiosis I. The remaining DSBs are repaired as noncrossovers (with nonreciprocal exchange between homologous chromosomes) or from the sister chromatid (Bishop and Zickler, 2004; Baudat and de Massy, 2007; Mancera et al., 2008). At least one CO per homologous chromosome pair is needed for the correct segregation of homologs during the first meiotic division. Despite the presence of a sister chromatid in close proximity, the meiotic DNA repair machinery has to be directed, at least in some cases,

[1] These authors contributed equally to this work.
[2] Current address: Group of Reproductive Development and Apomixis, Laboratorio Nacional de Genómica para la Biodiversidad, Centro de Investigación y de Estudios Avanzados del Instituto Politécnico Nacional, Km 9.6 Libramiento Norte Carretera Irapuato-León C.P. 36821, Irapuato, Guanajuato, Mexico.
[3] Current address: Institut Curie/Centre de Recherche, Unité Mixte de Recherche 218, Pavillon Pasteur, F-75248 Paris, France.
[4] Address correspondence to peter.schloegelhofer@univie.ac.at.
The authors responsible for distribution of materials integral to the findings presented in this article in accordance with the policy described in the Instructions for Authors (www.plantcell.org) are: Peter Schlögelhofer (peter.schloegelhofer@univie.ac.at) and Mathilde Grelon (mathilde.grelon@versailles.inra.fr).
[W] Online version contains Web-only data.
www.plantcell.org/cgi/doi/10.1105/tpc.113.118521

to the homologous chromosome as a repair template. The molecular mechanisms underlying this promotion of interhomologous (IH) and the possible correlated suppression of intersister (IS) recombination are still poorly understood (De Massy et al., 1994; Pâques and Haber, 1999; Niu et al., 2005; Callender and Hollingsworth, 2010; Goldfarb and Lichten, 2010).

Two proteins play a major role in establishing the nucleoprotein filament and finding the target sequence: the RecA homologs RADIATION SENSITIVE51 (Rad51) and DISRUPTED MEIOTIC cDNA1 (Dmc1) (Bishop et al., 1992; Shinohara et al., 1992, 1997; Ogawa et al., 1993; Bishop, 1994). Rad51 is involved in both mitotic and meiotic recombination, whereas Dmc1 is exclusively a meiotic player (Bishop et al., 1992; Tashiro et al., 1996, 2000; Yamamoto et al., 1996; Klimyuk and Jones, 1997) (reviewed in Masson and West, 2001; Li and Ma, 2006). It has been demonstrated that during meiosis, Rad51 and Dmc1 function in independent DNA repair pathways and that their loading onto replication protein A–coated ssDNA is supported by distinct sets of proteins (Bishop, 1994; Dresser et al., 1997; Gasior et al., 2001; Hayase et al., 2004; Li et al., 2004; Lao et al., 2008).

During wild-type meiosis, DMC1-mediated IH DNA repair appears to be the predominant pathway, with RAD51 just having a supportive role, as recently shown for yeast (*Saccharomyces cerevisiae*) and plants (Garcia et al., 2011; Cloud et al., 2012). In the absence of DMC1, RAD51 can promote efficient meiotic IS DNA repair in *Arabidopsis thaliana* (Couteau et al., 1999; Vignard et al., 2007; De Muyt et al., 2009) and in yeast when the Rad51 inhibitor High copy suppressor of Red1 (Hed1) is not present (Busygina et al., 2008). These data are in line with our recent findings that during meiosis in *Arabidopsis*, RAD51 and DMC1 form distinct functional units, also represented in nonoverlapping nuclear foci (Kurzbauer et al., 2012). Purified DMC1 and RAD51 from human and budding yeast seem not distinct from each other with respect to their biochemical properties. Both proteins form right-handed helical filaments on ssDNA in an ATP-dependent manner and catalyze homologous DNA pairing and strand exchange reaction (Shinohara et al., 1992; Ogawa et al., 1993; Benson et al., 1994; Sung, 1994; Baumann et al., 1996; Li et al., 1997; Masson et al., 1999; Hong et al., 2001; Sehorn et al., 2004; Yu and Egelman, 2010). By contrast, fission yeast (*Schizosaccharomyces pombe*) Rad51 and Dmc1 proteins differ from each other in in vitro assays with respect to the polarity of strand exchange reactions they support (Murayama et al., 2011). Generally, it has been suggested that a set of distinct accessory proteins that modulate the activity of Dmc1 or Rad51 is responsible for the observed differences in their meiotic function (Sheridan and Bishop, 2006; Sheridan et al., 2008; Kagawa and Kurumizaka, 2010; Dray et al., 2011).

The proteins HOMOLOGOUS-PAIRING PROTEIN2 (Hop2) and MEIOTIC NUCLEAR DIVISION PROTEIN1 (Mnd1) have been identified in yeast as factors supporting homologous chromosome pairing and meiotic DSB repair (Leu et al., 1998; Tsubouchi and Roeder, 2002; Chen et al., 2004). Analyses in yeast have shown that both *mnd1* and *hop2* mutants initiate recombination, but do not form heteroduplex DNA or double Holliday junctions, accumulate Dmc1 and Rad51, and lead to severe DNA repair defects, suggesting that they are involved in strand invasion. These mutants arrest in prophase I due to DNA damage checkpoint activation (Leu et al., 1998; Gerton and DeRisi, 2002; Tsubouchi and Roeder, 2002; Chen et al., 2004; Zierhut et al., 2004). Furthermore, in yeast, Dmc1 directs meiotic repair to the homologous chromosome only in the presence of Mnd1 and Hop2 (Zierhut et al., 2004). Recent results demonstrate that the Hop2/Mnd1 protein complex can efficiently condensate double-stranded DNA (dsDNA) to support strand invasion as a key step in stimulating association of the ssDNA-nucleoprotein filament with the dsDNA (Pezza et al., 2010). Mammalian HOP2/MND1 complexes can interact with DMC1 but also with RAD51 in vitro, stimulating the strand exchange activities of both proteins, 35-fold or 10-fold, respectively, but do not show strand exchange activity alone (Petukhova et al., 2005; Enomoto et al., 2006).

The involvement of the HOP2/MND1 complex in meiotic DSB repair has also been observed in *Arabidopsis thaliana*, since null mutants of *HOP2* and *MND1* lead to chromosome fragmentation and sterility. Nevertheless, the *Arabidopsis* HOP2/MND1 complex has not been shown to be involved in the promotion of IH repair via a DMC1-directed pathway since both IH and IS DNA repair are dysfunctional in the absence of any of these two proteins (Schommer et al., 2003; Kerzendorfer et al., 2006; Stronghill et al., 2010). Recently, we identified two mutant alleles of *Arabidopsis HOP2* (De Muyt et al., 2009) that differ from the already characterized *hop2-1* null mutant allele (previously named *ahp2-1*; renamed *hop2-1* for nomenclature consistency; Schommer et al., 2003). *hop2-1* mutants exhibit strong DNA fragmentation during meiosis I, while the two newly identified alleles show random segregation of univalents during meiosis I (accompanied by only limited chromosome fragmentation), reminiscent of the defects observed in *Arabidopsis dmc1* mutants. This led to the assumption that in these two mutants, IH bias is lost and the repair of meiotic DSBs occurs exclusively via the sister chromatid. Here, we present molecular and biochemical analyses demonstrating that plant HOP2 protein and its heterodimeric partner MND1 need to form functional complexes at sufficient levels to support IH DNA repair. Genetic analyses revealed that the HOP2/MND1 complex is dispensable for RAD51-mediated IS DNA repair in the absence of DMC1. In the presence of DMC1, HOP2/MND1 becomes an essential factor: At low levels, it indirectly allows RAD51-mediated IS repair and only at high levels does it support DMC1 driven IH repair.

RESULTS

In a forward-genetic meiotic mutant screen in *Arabidopsis*, two mutant alleles of *HOP2*, *hop2-2* (initially named *eyu48*) and *hop2-3* (initially named *exi5*), were previously identified (De Muyt et al., 2009). The mutants can be recognized by their reduced silique length and reduced seed set, while their overall appearance is indistinguishable from the wild type. Only 1.6 $\pm$ 0.75 (n = 1099 siliques) seeds per silique (3.8% of the wild type) were observed in *hop2-2* and 0.84 $\pm$ 0.53 (n = 825 siliques) seeds per silique (2.03% of the wild type) were observed in *hop2-3*. This is in strong contrast with the observations made in the previously published *hop2-1* null mutant allele (Schommer et al., 2003), which produces only 0.005 $\pm$ 0.01 (n = 886 siliques) seeds per silique (0.01% of the wild type). To understand these differences and their molecular basis, we first analyzed the meiotic progression of all the mutants in detail.

hop2-2 and *hop2-3* Show a High Incidence of Univalents in Meiosis I

We could detect strong abnormalities in meiotic progression in all *Arabidopsis hop2* mutants investigated in this study. First, normal chromosome pairing was not observed during prophase I of male meiosis in any of the studied alleles (Figures 1Ae and 1Ai to 1Aa) (Schommer et al., 2003; Stronghill et al., 2010). As described before (Schommer et al., 2003), severe chromosomal defects (chromosome bridges and DNA fragmentation) could be observed from anaphase I to the end of meiosis in *hop2-1* (Figures 1Af to 1Ah) in a large majority of the meiotic cells (Figure 1B, 82%, $n = 39$). In clear contrast, *hop2-2* meiocytes showed hardly any chromosome fragmentation or chromosome bridges, but instead exhibited intact chromosomes (Figures 1Aj and 1Ak) in the vast majority of the cells observed (Figure 1B, 86%, $n = 154$,). Nevertheless, contrary to the wild type (Figure 1Ab), very few bivalents but a majority of univalents were observed among *hop2-2* metaphase cells. On average, we counted 0.5 bivalent/meiocytes ($n = 133$), while the wild type always shows five bivalents per cell. For the remaining cells (21 out of 154), no major chromosomal defects were observed but chromosomes display poorly condensed chromatin or occurrence of a reduced number of chromosome fragments and were classified as intermediate class in Figure 1B.

In *hop2-3* meiocytes, the situation is intermediate, with 55% of the cells showing intact chromosomes (mean number of bivalent per cell of 0.3 ± 0.1; $n = 95$) and 41% showing mild chromosomal defects (Figure 1B). For *hop2-2* and *hop2-3* mutants, random segregation of the univalents at anaphase I and subsequent sister chromatid segregation at meiosis II yielded unbalanced pools of chromosomes at the end of meiosis (Figure 1Al), contrary to the situation in the wild type where the balanced segregation of homologous chromosomes during meiosis I and the subsequent sister chromatid segregation at meiosis II generates four haploid daughter cells (Figures 1Ac and 1Ad).

Reciprocal Partial Complementation of *hop2-2* and *hop2-3*

Interestingly, we found that in heteroallelic *hop2-2/hop2-3* plants, chromosome fragmentation and bridges were completely suppressed (see Supplemental Figure 1 online). In addition, the level of bivalent formation was significantly increased when compared with each single mutant line ($P = 9.5 \times 10^{-12}$ and $P = 3.8 \times 10^{-10}$). While *hop2-2* and *hop2-3* have a mean number of 0.3 bivalents per cell, the *hop2-2/hop2-3* line shows 1 ± 0.1 bivalents per cell ($n = 91$). This increase in bivalent formation is also followed by an increase in fertility, with an average number of 8.1 seeds per silique (± 1.3, $n = 29$; 9.2% of the wild type). This reciprocal (partial) complementation suggested that different aspects of gene regulation or protein functions are affected in the two mutant alleles.

hop2-2 and *hop2-3* Represent Different Hypomorphic Alleles of *HOP2*

To understand the differences between *hop2-1* and the alleles *hop2-2* and *hop2-3*, we characterized the mutant alleles in detail. Sequencing of the *HOP2* gene in these alleles revealed the nature of each mutation. The original *hop2-1* null-mutant (in the Landsberg *erecta* [*Ler*] background) has a T-DNA insertion in exon 4, does not produce functional mRNA, and lacks HOP2 protein (Figure 2A) (Schommer et al., 2003; Stronghill et al., 2010). The *hop2-2* allele has a 147-bp deletion 101 bp upstream of the start codon of the *HOP2* gene (Figure 2A). The *hop2-3* allele has a deletion of 128 bp between exon 4 and exon 5. The deletion in *hop2-3* leads to a transcript lacking parts of sequences from exon 4 and 5 and all of intron 4 but keeping the translational phase of the coding sequence (CDS; Figures 2A and 2D; see Supplemental Figure 2 online).

We analyzed the expression levels of *HOP2* in the four mutants using material from young flower buds by RT-PCR using three different primer sets (Figure 2B). As described previously, the 5′ end and the 3′ end of the *HOP2* mRNA could be identified in the *hop2-1* mutants, but a transcript spanning the T-DNA insertion site could not (Schommer et al., 2003).

For the *hop2-3* allele, we observed transcript levels as in the wild type. It should be noted that in *hop2-3* mutants, the corresponding transcript is 42 nucleotides shorter due to the deletion described above (Figure 2B). The nature of the *hop2-3* mRNA has been confirmed by sequencing. We reasoned that the shortened mRNA leads to the expression of a HOP2 protein variant that lacks 14 amino acids (positions 123 to 136; UniProtKB Q9FX64) in its putative coiled coil domain (Figure 2D) and that it may be this truncated protein that causes the observed phenotype in *hop2-3* mutant plants.

In *hop2-2* mutants, we observed drastically reduced mRNA levels of HOP2 (Figures 2B and 2C). Quantitative RT-PCR showed that the *HOP2* mRNA is at least fivefold decreased when evaluating the 5′ part of mRNA and ~30-fold decreased when evaluating the 3′ part of the mRNA in *hop2-2* mutants. The low abundance of the 3′ part of the mRNA in *hop2-2* mutants may indicate mRNA truncation or instability. We reasoned that the observed phenotype in *hop2-2* has to be attributed to the severely reduced *HOP2* transcript levels and the anticipated lower HOP2 protein levels.

The High Incidence of Univalents in *hop2-2* and *hop2-3* Is Not Due to a Failure to Generate DSBs

In order to understand if the high incidence of univalents and the decrease of chiasma numbers observed in *hop2-2* and *hop2-3* meiocytes was due to reduction of DNA DSBs, we generated double mutants of *hop2-2* and *hop2-3* with *mre11-3* (Puizina et al., 2004) and *rad51* (Li et al., 2004) mutants. Both MEIOTIC RECOMBINATION11 (MRE11) and RAD51 are well-studied proteins, essential for meiotic progression in plants and other organisms (Cao et al., 1990; Shinohara et al., 1992; Haaf et al., 1995; Muris et al., 1997; Li et al., 2004; Puizina et al., 2004). MRE11 is involved in early steps of SPO11-generated DSB processing, and RAD51, as discussed above, is needed in the strand invasion process during DNA repair. Since DSB formation is not affected in *Arabidopsis mre11* and *rad51* mutants, the respective DNA repair defects lead to chromosome fragmentation and sterility. If the *hop2-2* and *hop2-3* alleles affect DSB formation, we reasoned that the DNA fragmentation observed in *mre11-3* and *rad51* mutants should be alleviated in the *hop2-2 mre11*, *hop2-3 mre11*, *hop2-2 rad51*, and *hop2-3 rad51* double mutants. Since this is not the case (see Supplemental Figure 3 online), we can exclude major defects in DSB formation in both *hop2* mutant

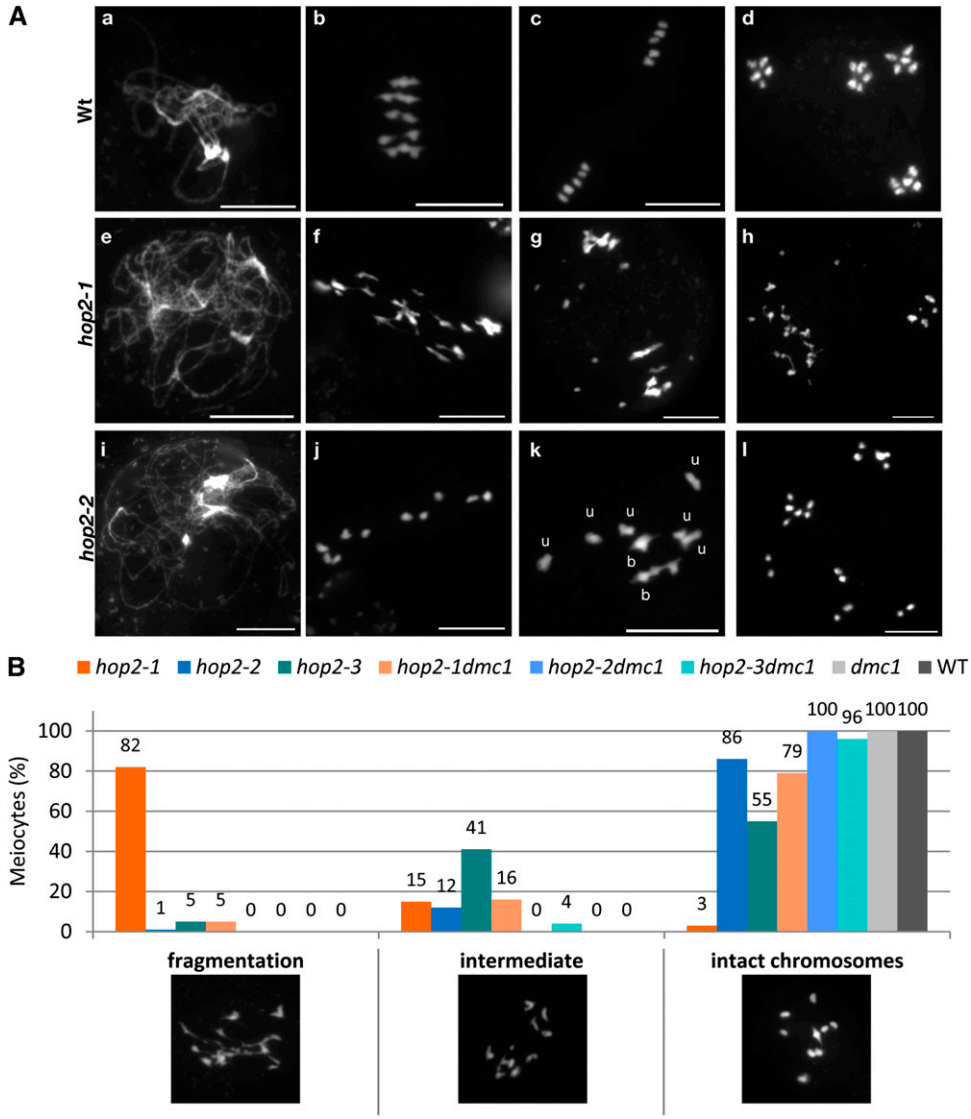

Figure 1. Meiotic Progression in *hop2* Mutants.

(A) 4′,6-Diamidino-2-phenylindole staining of chromosomes of wild-type (Wt; **[a]** to **[d]**), *hop2-1* (**[e]** to **[h]**), and *hop2-2* (**[i]** to **[l]**) pollen mother cells. **(a)**, **(e)**, and **(i)**, Pachytene/pachytene-like stage; **(b)**, **(f)**, **(j)**, and **(k)**, metaphase I–anaphase I transition; **(c)** and **(g)**, metaphase II; **(d)**, **(h)**, and **(l)**, end of anaphase II. While full synapsis was achieved at pachytene in the wild type **(a)**, no evidence of synapsis could be observed in any of the three *hop2* mutant lines (shown here for *hop2-1* in **[e]** and *hop2-2* in **[i]**). At metaphase I in the wild type, five bivalents were always observed aligned on the metaphase plate **(b)**. Homologous chromosomes segregated during anaphase I, generating two pools of five chromosomes **(c)**. Then, during the second meiotic division, sister chromatids were separated, producing four haploid cells **(d)**. By contrast, during *hop2-1* meiosis **(f)**, severe chromosomal defects (fragmentation and chromosome bridges) were observed at anaphase I **(f)** and anaphase II **(g)**, yielding aberrant meiotic products **(h)**. In *hop2-2* (**[j]** to **[l]**) and *hop2-3*, hardly any chromosomal defects could be observed; instead, a mixture of intact univalents and bivalents could be seen (**[j]**, 10 univalents; **[k]**, six univalents and two bivalents). Random segregation of these univalents at anaphase I (**[j]** and **[k]**) and the subsequent sister chromatid segregation at meiosis II (data not shown) yielded unbalanced pools of chromosomes at the end of meiosis **(l)** instead of the four pools of five chromosomes observed in the wild type **(d)**. u, univalent; b, bivalent. Bars = 10 μm.

(B) *dmc1* suppresses the DNA repair defects observed in *hop2-1*, *hop2-2*, and *hop2-3* mutants. In *hop2-1*, a large majority of meiocytes showed drastic chromosomal defects (fragmentation and chromosome bridges) at metaphase I–anaphase I transition. By contrast, *hop2-2* cells predominantly present intact chromosomes (86%). In *hop2-3* meiocytes, the situation is intermediate with 55% of the cells showing no DNA fragmentation and 41% showing mild chromosomal defects (“intermediate” class). The severe chromosome fragmentation observed in *hop2-1* mutants is largely suppressed by the *dmc1* mutation. The limited chromosome fragmentation observed in *hop2-2* and *hop2-3* mutants is nearly completely suppressed by the *dmc1* mutation.

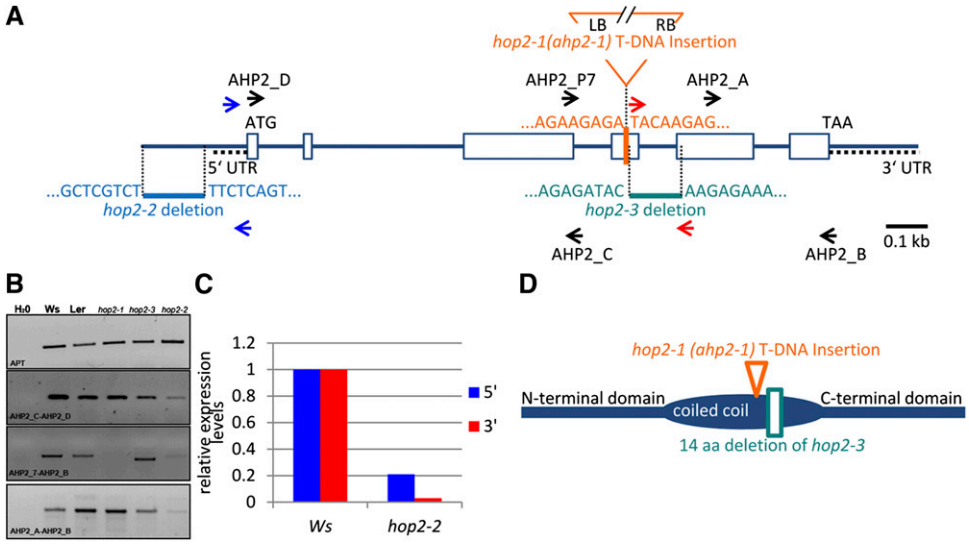

Figure 2. Molecular Analysis of *HOP2* Alleles.

(A) Schematic representation of the *HOP2(AHP2)* gene and three mutant alleles. Open boxes represent exons, ATG and TAA encompass the open reading frame. The inverted triangle in orange shows the position of the T-DNA insertion in *hop2-1* (the renamed *ahp2-1* allele described in Schommer et al., 2003). Text and symbols in light blue indicate the 147-bp deletion in the promoter region of the hypomorphic *hop2-2* allele. Text and symbols in turquoise indicate the 128-bp deletion in the hypomorphic *hop2-3* allele.

(B) RT-PCR analysis of *HOP2* and *hop2* mutant allele expression in young flower buds. A *HOP2* transcript spanning the T-DNA insertion site was not detected in *hop2-1* (primers AHP2_P7 and AHP2_B), while sequences upstream (AHP2_C and AHP2_D primers) and downstream (AHP2_A and AHP2_B primers) of the insertion could be amplified. In *hop2-2*, reduced levels of mRNA can be detected with all primer combinations. In *hop2-3*, normal levels of mRNA can be detected with all primer combinations. Nevertheless, an expected shorter transcript is amplified when using primers AHP2_P7 and AHP2_B, which span the genomic deletion of *hop2-3*. The mRNA/cDNA of the phosphoribosyltransferase (*APT*) gene was used for normalization. The corresponding wild-type controls were from ecotypes Ws and L*er*.

(C) Quantitative RT-PCR of *HOP2* and *hop2-2* mutant expression in young flower buds. Primers were designed to determine expression levels of the 5′ part of the mRNA (blue arrows in **[A]**; blue bar) and the 3′ part of mRNA (red arrows in **[A]**; red bar). All values were normalized to *Actin2/7* gene expression. The mRNA levels detected in *hop2-2* mutants are strongly decreased compared with the wild type: approximately fivefold decreased when evaluating the 5′ part of mRNA (green bars) and ~30-fold decreased when evaluating the 3′ part of the mRNA. The corresponding wild-type control was from ecotype Ws.

(D) Schematic representation of the anticipated HOP2 protein and its hypomorphic variant. The HOP2 wild-type protein is structured into an N-terminal domain, a putative coiled coil region, and a C-terminal domain. *hop2-1* plants do not express the protein (Stronghill et al., 2010). Plants carrying the hypomorphic *hop2-2* allele produce very low levels of the mRNA and anticipated very low levels of HOP2 protein. The deletion in *hop2-3* leads to expression of an mRNA variant, anticipated to encode a protein variant that lacks 14 amino acids (position 123 to 136 of the wild-type protein) within the coiled coil region of the protein.

alleles. In addition, these results suggested that RAD51 is instrumental for DNA repair in *hop2-2* and *hop2-3* mutants.

dmc1 Suppresses the DNA Repair Defects Observed in *hop2-1*, *hop2-2*, and *hop2-3* Mutants

The observed phenotype in *hop2-2* and *hop2-3* mutants is reminiscent of the defects observed in the *Arabidopsis dmc1* mutants (Couteau et al., 1999), in which meiotic DSBs are formed but repaired without CO outcome. It has been proposed earlier that in *dmc1* mutants, meiotic DNA repair depends on RAD51 and that the sister chromatid is used as a repair template (Zenvirth et al., 1997; Couteau et al., 1999; Kurzbauer et al., 2012; Wijnker et al., 2012). Accordingly, *dmc1 rad51* mutants show severe chromosome fragmentation during meiosis (Siaud et al., 2004; Vignard et al., 2007). To understand the impact of DMC1 on meiotic DNA repair in *hop2* mutants, various double mutants have been generated and analyzed.

While in *hop2-2* and *hop2-3*, some chromosomal defects are observed, *dmc1* mutants display 100% intact chromosomes (Figure 1B). Double mutants of *hop2-2 dmc1* (n = 67 cells) and *hop2-3 dmc1* (n = 67 cells) resemble *dmc1* single mutants with a nearly complete suppression of the chromosomal defects observed in the *hop2-2* and *hop2-3* single mutants (Figure 1B).

By contrast, *hop2-1* single mutants show, as outlined above, severe chromosome fragmentation. Interestingly, this severe fragmentation could largely be suppressed by the introduction of the *dmc1* mutant allele (Figure 1B). Accordingly, 79% (n = 87) of all observed cells do not show any DNA fragmentation (with only intact univalents present) in *hop2-1 dmc1* double mutants, as opposed to the occurrence of DNA fragmentation in 82% of the *hop2-1* cells observed (Figure 1B). Moreover, in *hop2-1 dmc1* double mutants, 2.08% of seeds per silique were generated (compared with the wild type; n = 1028 siliques), in clear contrast with *hop2-1* single mutants (0.01% seeds per silique compared

with the wild type; see above) and similar to *dmc1* mutant plants (3.2% seeds per silique compared with the wild type; *n* = 791 siliques). Furthermore, in *hop2-1 mnd1 dmc1* triple mutants, 2.35% of seeds per silique were generated (compared with the wild type; *n* = 312 siliques), similar to *dmc1* single and *hop2-1 dmc1* double mutants. This implies that HOP2 (and the HOP2/MND1 complex) is largely dispensable for RAD51-mediated meiotic DNA repair in the *dmc1* mutant background. It furthermore implies that a lack of HOP2 protein (*hop2-1* null mutant allele) impedes DNA repair only in the presence of DMC1 protein. The *HOP2* alleles *hop2-2* and *hop2-3*, while anticipated to be compromised in optimally supporting DMC1-mediated DNA repair, may allow DNA repair to take place in a RAD51-dependent manner using the sister chromatid as a repair template, even in the presence of functional DMC1 protein.

MND1 Is Required for DNA Repair in *hop2-2* and *hop2-3* Mutant Alleles but Its Loading on Meiotic Chromatin Is Reduced in *hop2-2*

In order to gain more insight into the origin of the meiotic defects observed in the *hop2* allelic series, we performed immunohistochemical detection of MND1 on meiotic chromatin spreads together with ASYNAPTIC1 (ASY1), a protein associated with the axial elements of meiotic chromosomes that allows meiotic progression to be followed (Armstrong et al., 2002). In wild-type *Arabidopsis* meiosis, MND1 can be detected on chromatin loops during meiotic prophase, as shown in Figure 3A. Besides, MND1 loading onto chromatin was shown to be dependent on HOP2 (Vignard et al., 2007). We confirmed this observation, since no MND1 signal could be detected above background in the null allele *hop2-1* (Figure 3C). In clear contrast, we detected an MND1 signal indistinguishable from the wild type in the *hop2-3* allele (Figure 3E; *n* = 159), while in *hop2-2* mutants, the MND1 signal was severely reduced (Figure 3D; *n* = 131). This latter result further corroborated that different functional aspects of HOP2 are compromised in the *hop2-2* and *hop2-3* mutants.

To confirm the presence and importance of MND1 in *hop2-2* and *hop2-3* mutant plants genetically, we introgressed the *mnd1* mutation (Kerzendorfer et al., 2006) into the *hop2* mutants (Figures 3F to 3J). In the absence of the MND1 protein, meiotic DSB repair is highly perturbed and *mnd1* mutant meiosis is similar to *hop2-1* meiosis, showing strong chromosome fragmentation and entanglements (cf. Figures 3G and 1Af). We found that *mnd1* is epistatic to *hop2-2* and *hop2-3* (Figures 3I and 3J), indicating that the DSB repair observed in the two *hop2-2* and *hop2-3* alleles depends on the presence of MND1. This underlines the importance of the MND1 protein and its protein function in combination with the *hop2-2* and *hop2-3* alleles.

DMC1 and RAD51 Foci Numbers in *hop2* Mutant Alleles Are Comparable to the Wild Type

Since MND1 is less abundant in the *hop2-2* mutant allele, we reasoned that this may lead to altered stability of DMC1-coated nucleoprotein filaments, manifested by altered numbers of DMC1 recombinase foci counted on meiotic spreads. Previously we, and others, established that loading of DMC1 requires RAD51 (Bishop, 1994; Cloud et al., 2012; Kurzbauer et al., 2012) and that in an *Arabidopsis mnd1* mutant, DMC1 foci accumulate in a RAD51-dependent manner (324 ± 103 foci in *mnd1* [*n* = 22] versus 234 foci ± 89 [*n* = 28] in the wild type; P = 0.0001) (Vignard et al., 2007). At that time, we inferred that DMC1-coated nucleoprotein filaments will not be supported in strand invasion reactions in *mnd1* mutants; therefore, their turnover may be decreased, resulting in more DMC1 foci on meiotic chromatin. In this sense, we anticipated a similar

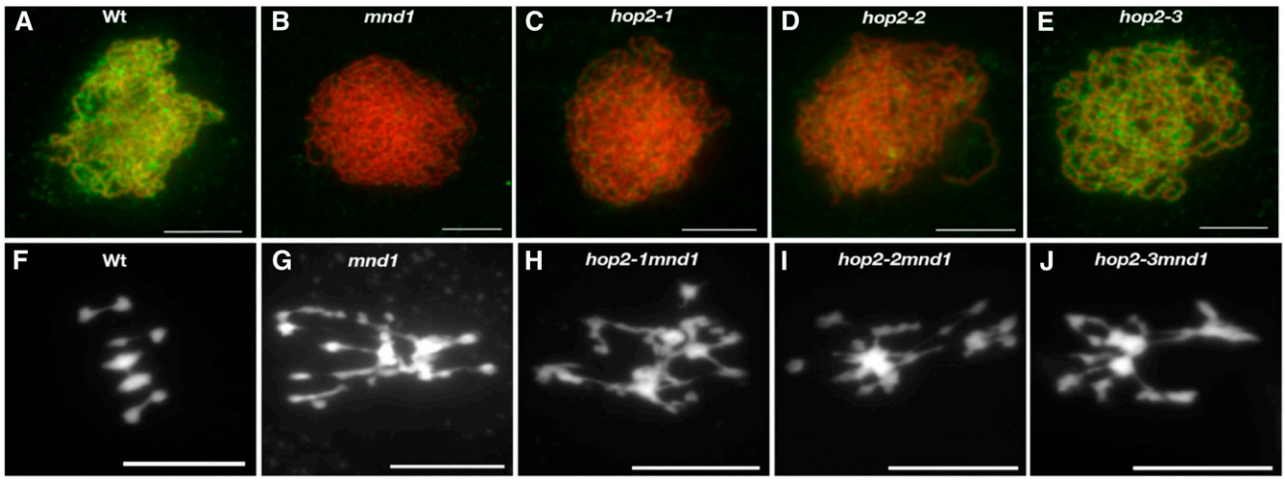

Figure 3. The Formation of MND1 Foci Is Normal in *hop2-3*, Reduced in *hop2-2*, and Abolished in *hop2-1* Mutants.

(A) to **(E)** Coimmunolocalization of ASY1 (red) and MND1 (green) in wild-type (Wt; **[A]**), *mnd1* **(B)**, and *hop2* mutant meiocytes (**[C]** to **[E]**). In accordance with our previous studies (Vignard et al., 2007), no MND1 foci were detected in *mnd1* or *hop2-1* meiocytes (**[B]** and **[C]**). By contrast, MND1 signal appeared normal in *hop2-3* mutant meiocytes **(E)** and reduced in *hop2-2* meiocytes **(D)**. Bars = 5 μm.

(F) to **(J)** 4′,6-Diamidino-2-phenylindole staining of metaphase I pollen mother cells in the wild type **(F)**, *mnd1* **(G)**, *hop2-1 mnd1* **(H)**, *hop2-2 mnd1* **(I)**, and *hop2-3 mnd1* **(J)** mutants. Bars = 10 μm.

increase in DMC1 foci numbers in *hop2-1* and to a certain extent in *hop2-2* mutants. To follow DMC1 focus formation throughout meiosis, coimmunolocalization was performed with antibodies that recognize the meiotic proteins ASY1 and DMC1 (Armstrong et al., 2002; Chelysheva et al., 2007). DMC1 foci appear at late leptotene/early zygotene, reaching an average of 234 foci (±89, $n = 28$) per nucleus and disappear by pachytene. The mean number of DMC1 foci is not statistically different between the wild type and *hop2-2* (205 ± 49, $n = 17$) ($P = 0.4533$) or between the wild type and *hop2-3* (227 ± 89, $n = 21$) ($P = 0.6312$). In the case of the null allele *hop2-1*, we counted 182 (±47, $n = 17$) DMC1 foci (Figure 4; see Supplemental Figure 4A online). This number is slightly but significantly smaller ($P = 0.0316$) when compared with foci counts in the wild type (234 foci ± 89; $n = 28$).

RAD51 foci were counted in leptotene/early zygotene and reached an average number of 224 (±78, $n = 35$) in wild-type meiocytes. The mean number of RAD51 foci is not statistically different between the wild type and *hop2-1* (188 ± 41, $n = 9$) ($P = 0.2801$), *mnd1* (210 ± 41, $n = 20$) ($P = 0.5157$), and *hop2-3* (216 ± 56, $n = 25$) ($P = 0.9442$). In the case of *hop2-2*, we counted 169 (±39, $n = 14$) RAD51 foci, a value significantly different from the wild type ($P = 0.015$) (Figure 4; see Supplemental Figure 4B online).

Despite the slight reduction of RAD51 and DMC1 foci, in some *hop2* alleles, RAD51 and DMC1 loading or turnover does not appear to be strongly affected. Following our observations of the differential effects of the *mnd1* and *hop2-1* null mutant alleles on DMC1 foci numbers (but not on RAD51 foci numbers), we infer that MND1 and HOP2 proteins may have some different molecular functions, even though they may form a functional unit for most of their tasks.

HOP2-3/MND1 Complex Has a Reduced Thermal Stability

We were interested in determining whether the anticipated, truncated HOP2-3 protein has retained its full functionality or, alternatively, has lost parts of its function and may therefore be impaired in supporting IH DNA repair processes. To test protein function directly, we heterologously expressed and purified protein complexes comprising either MND1 and the full-length HOP2 or MND1 and the internally truncated HOP2-3. We furthermore characterized the molecular function of other domains of the HOP2 and MND1 proteins, using different truncated protein variants.

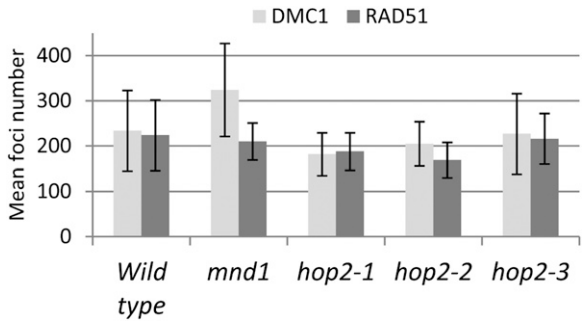

Figure 4. No Major Differences in DMC1 and RAD51 Foci Numbers in All *hop2* Mutant Alleles.

Chromosome spreads of *Arabidopsis* meiocytes from the wild type, *mnd1*, *hop2-1*, *hop2-2*, and *hop2-3* mutants were stained with an α-ASY1 antibody and an α-RAD51 or α-DMC1 antibody (see Supplemental Figure 4 online). Foci numbers were determined and the counts blotted. While DMC1 and RAD51 foci numbers are not dramatically changed in all *hop2* mutant alleles, the DMC1 foci number in *mnd1* is significantly higher than in the wild type and all other mutant lines (Vignard et al., 2007). Please refer to text for more details.

First, we coexpressed untagged MND1 and (6xHis-) tagged HOP2 and HOP2 variants in *Escherichia coli* cells and copurified proteins with columns, exclusively retaining His-tagged proteins. MND1 and HOP2 as well as MND1 and the HOP2-3 protein variant showed tight association and were coeluted (Figure 5A). While the interaction between MND1 and HOP2 could be demonstrated directly by staining proteins in gels, proving the interaction between MND1 and HOP2-3 was complicated due to their similar size. We therefore blotted the proteins on a membrane following separation on a protein gel and thereafter probed the membrane with specific antibodies directed against either MND1 or HOP2 (see Supplemental Figure 5 online). Further experiments with truncated protein versions of MND1 and HOP2 demonstrated that the coiled coil domains of both partners are sufficient for formation of the protein complex (see Supplemental Figure 6 online). Since the HOP2-3 protein has a 20% shortened coiled coil domain lacking two complete heptad repeats, we reasoned that the interaction between HOP2-3 and MND1 may be weakened compared with that of the wild-type proteins.

We therefore tested the thermal stability of the recombinant protein complexes by electronic circular dichroism (ECD) spectroscopy. Figure 5B depicts ECD spectra in the far-UV region for HOP2/MND1 and HOP2-3/MND1 in their native state, denatured state, and partially refolded state. The overall secondary structure according to the ECD spectra for both complexes is predominantly α-helical, with typical minima at 208 and 222 nm in their ellipticity (Kelly et al., 2005; Greenfield, 2006). Upon unfolding of both complexes (T = 85°C), some residual ellipticity remained. In the unfolded state, spectra show ellipticity minima at around 200 nm (characteristic minimum for random coil conformation) and a shoulder at around 220 nm (residual ellipticity from α-helices). ECD spectra recorded at 20°C after heating and cooling of the protein complexes were indicative of partially refolded protein complexes.

We followed temperature-mediated unfolding at 222 nm (reflecting melting of secondary structure, mainly α-helices) (Figure 5C). In HOP2/MND1, α-helices melted between 30 and 40°C (calculated $T_m = 34$°C) in a simple two-state transition. There was a clear linear relationship between the equilibrium constants and the reciprocal temperature, allowing the calculation of the van't Hoff enthalpy for this transition, which was 212 ± 9 kJ mol^{-1}. HOP2-3/MND1 melted at significantly lower temperatures between 20 and 30°C (calculated $T_m = 25$°C). The melting of the secondary structures followed a two-state transition and allowed the calculation of the van't Hoff enthalpy, which was 272 ± 15 kJ mol^{-1}. These results demonstrate that the HOP2-3/MND1 protein complex is less stable than the wild-type complex.

The N Termini of Both HOP2 and MND1 Are Required for DNA Binding

Following the tests above, we were interested in determining whether the altered stability of the HOP2-3/MND1 complex has

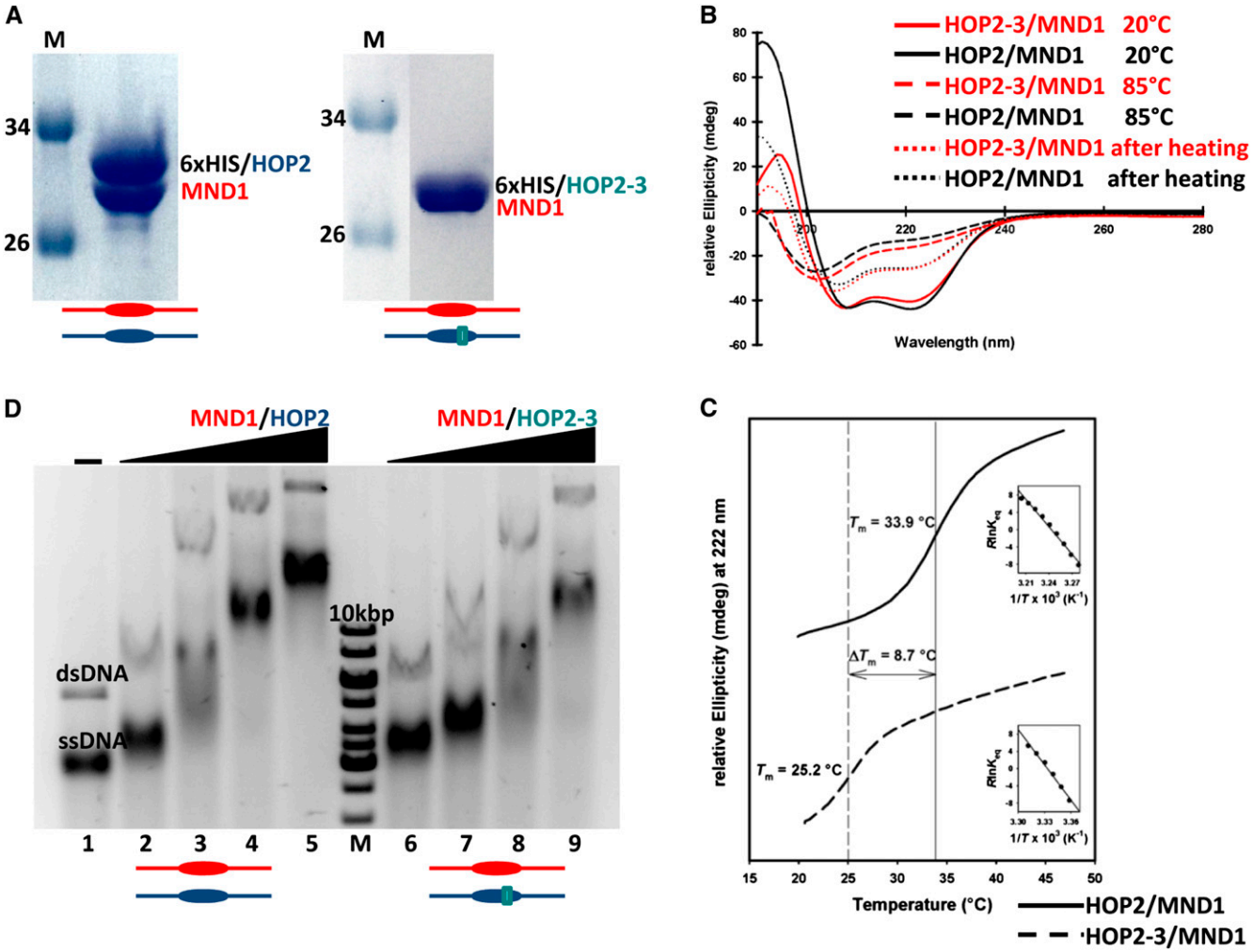

Figure 5. HOP2-3/MND1 Protein Complex Is Less Stable Than the HOP2/MND1 Complex.

(A) HOP2 and HOP2-3 form complexes with MND1. SDS-PAGE and Coomassie blue staining of the coexpressed and copurified recombinant HOP2/MND1 and the HOP2-3/MND1 complexes. HOP2 or HOP2-3 has been fused to a 6xHis-tag, which was used to purify HOP2 or HOP2-3 and to copurify MND1. Subsequent immunoblotting was performed to demonstrate the presence of both proteins (see Supplemental Figure 5 online).

(B) Temperature-mediated unfolding of the HOP2/MND1 and HOP2-3/MND1 protein complexes followed by ECD in the far UV. Conditions: 5 mM phosphate buffer, pH 7.7. Comparison of far-UV ECD spectra of HOP2/MND1 (black) and HOP2-3/MND1 (red) at 20°C (solid lines), 85°C (dashed lines), and 20°C after heating and cooling (dotted lines).

(C) Thermal unfolding of HOP2/MND1 (solid line) and HOP2-3/MND1 (dashed line) followed at 222 nm. The insets show the corresponding van't Hoff plots.

(D) DNA binding activities of the recombinant HOP2/MND1 and HOP2-3/MND1 protein complexes. Linearized PhiX174 Replication form I dsDNA and circular PhiX174 virion ssDNA were incubated with the following amounts of protein: 0, 1, 2.5, 5, 10 μM HOP2/MND1 for lanes 1 to 5 and 1, 2.5, 5, and 10 μM HOP2-3/MND1 for lanes 6 to 9. Reactions were loaded and separated on a 0.8% agarose gel and stained with ethidium bromide.

Diagrams below the gel pictures (**[A]** and **[D]**) indicate the recombinant proteins: red, MND1; blue, HOP2 or HOP2-3; ellipsoids represent the putative coiled coil domains; the turquoise rectangle indicates the 14–amino acid deletion in the second half of the putative coiled coil region in HOP2-3. M, Fermentas prestained protein ladder (numbers indicate molecular mass in kilodaltons). The calculated molecular weight for MND1 is 26.5 kD, for 6xHIS/HOP2-3 is 26.3 kD, and for 6xHIS/HOP2 is 28 kD.

an impact on its function. First, we tested DNA binding and, furthermore, which domains of the HOP2/MND1 complex are important for DNA binding. As demonstrated before (Chen et al., 2004; Pezza et al., 2006; Ploquin et al., 2007) for purified HOP2/MND1 proteins from other organisms, the *Arabidopsis* HOP2/MND1 protein complex binds ssDNA and dsDNA. The internally truncated HOP2-3 protein, in conjunction with MND1, binds to DNA as efficiently as the wild-type protein (Figure 5D). By contrast, the N termini of both HOP2 and MND1 are essential for ssDNA and dsDNA binding (see Supplemental Figures 7A and 7B online). Further experiments demonstrated that the Lys residue 58 in the N-terminal domain of HOP2 is crucial for DNA binding (see

Supplemental Figures 7F and 7G online and Supplemental References 1 online), thereby corroborating the results above. Furthermore, it is interesting to mention that neither the C termini of HOP2 nor MND1 are needed for the DNA interaction (see Supplemental Figures 7D and 7E online) and that the interacting coiled coil domains of HOP2 and MND1 cannot bind to DNA (see Supplemental Figure 7C online). The N-terminal domain of HOP2 alone, as well as the full-length HOP2, are not sufficient to mediate DNA binding efficiently (see Supplemental Figures 8 and 9 online). We furthermore determined that the HOP2/MND1 complex in plants forms a heterodimer, as shown before for other organisms (see Supplemental Figure 10 online) (Chen et al., 2004; Enomoto et al., 2006; Pezza et al., 2006; Ploquin et al., 2007). We therefore infer that HOP2 and MND1 operate cooperatively to build an efficient DNA binding platform consisting of their N-terminal domains.

HOP2-3/MND1 Fails to Activate DMC1-Mediated D-Loop Formation Efficiently

Next, we were interested in determining whether the interaction between the HOP2/MND1 complex variants and DMC1 was maintained, as this interaction was reported for several organisms (Petukhova et al., 2005; Ploquin et al., 2007). To this end, we performed affinity pull-down assays with HOP2/MND1 or HOP2-3/MND1, which were chemically cross-linked to *N*- hydroxysuccinimide beads. The resulting affinity resins were used to pull down recombinant DMC1 proteins (purified from Hi-5 insect cells). Alternatively, we coexpressed DMC1, MND1, and the respective HOP2 protein variants in *E. coli* and precipitated the complexes via the His tag on the HOP2 (variant) proteins. All three, the wild-type HOP2/MND1, the N-terminally truncated ΔN-HOP2/MND1, and the internally truncated HOP2-3/MND1 complexes, interacted with DMC1 (see Supplemental Figure 11 online and Supplemental References 1 online).

We were further interested in knowing whether the altered HOP2-3/MND1 complex would stimulate DMC1 activity as efficiently as wild-type HOP2/MND1. Recombinases like DMC1 polymerize on ssDNA to form nucleoprotein filaments that can locate a homologous dsDNA molecule, catalyze invasion, and form a DNA displacement loop called the D-loop. This activity can be measured in vitro with so-called D-loop assays. After several failed attempts to obtain sufficient amounts of soluble and active *Arabidopsis* DMC1 protein, we decided to use the two DMC1 protein variants from rice (*Oryza sativa*), which have been shown to be active in in vitro strand invasion assays (Sakane et al., 2008), to perform D-loop assays with purified rice DMC1A, DMC1B, HOP2/MND1, and HOP2-3/MND1 proteins (Figure 6). The Os-HOP2-3 protein variant exactly copies the anticipated *Arabidopsis* HOP2-3 protein variant (see Supplemental Methods

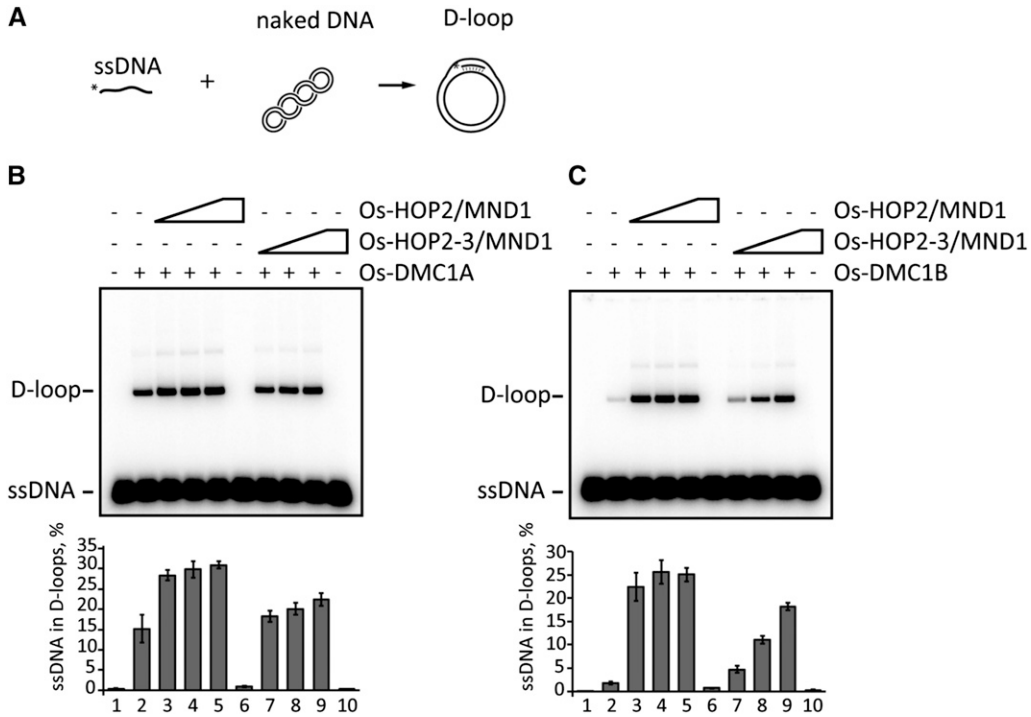

Figure 6. HOP2-3/MND1 Fails to Activate DMC1-Mediated D-Loop Formation Efficiently.

Principle of the D-loop assay **(A)**. A labeled ssDNA is first incubated with DMC1, followed by addition of HOP2/MND1 and then the supercoiled plasmid DNA to allow formation of D-loops. Reactions are stopped, proteins are removed, and DNA structures are separated by gel electrophoresis. Gel pictures showing D-loop assays employing rice DMC1A **(B)** or DMC1B **(C)** proteins with either the addition of wild-type HOP2/MND1 complex or HOP2-3/MND1 complex in increasing concentrations. All reactions were performed in triplicate and quantifications are shown below the gel pictures as percentages of ssDNA incorporated into D-loops.

online). The assays were performed in triplicate and show very robust results. While rice HOP2/MND1 stimulates Os-DMC1A 1.9- to 2.0-fold (depending on the concentration of HOP2/MND1) and Os-DMC1B 12.3- to 14.1-fold, the hypomorphic Os-HOP2-3 protein variant, in conjunction with Os-MND1, fails to do so efficiently and stimulates Os-DMC1A only 1.2- to 1.5-fold and Os-DMC1B only 2.6- to 10.0-fold. We therefore conclude that the suboptimal stability of the HOP2-3/MND1 complex compromises its ability to efficiently support DMC1-mediated strand invasion.

DISCUSSION

Meiotic RAD51 Function Is Independent of HOP2/MND1 and Is Negatively Regulated by DMC1

In vitro experiments with mammalian and yeast (*Saccharomyces cerevisiae and Schizosaccharomyces pombe*) proteins established that purified HOP2/MND1 stabilizes DMC1 nucleoprotein filaments and stimulates DMC1-mediated D-loop formation in vitro (Chen et al., 2004; Enomoto et al., 2006; Pezza et al., 2007; Ploquin et al., 2007). The mammalian complex can also stimulate RAD51 activity, but to a lesser extent than DMC1 activity (Petukhova et al., 2005), leading to the idea that the HOP2/MND1 complex is an accessory factor of DMC1 and, therefore, a crucial determinant of interhomolog DNA repair during meiosis. In plants, it was therefore surprising to find that in *mnd1* or *hop2* mutants, meiotic DNA repair would fail completely, while RAD51-mediated DNA repair via the sister chromatid was not compromised in a *dmc1* mutant (Schommer et al., 2003; Kerzendorfer et al., 2006). These results suggested that in plants, RAD51 needs to be supported by HOP2/MND1 during meiotic DNA repair.

However, our analysis revealed that the DNA repair defect observed in *hop2-1* null mutants can be largely suppressed by the introgression of a *dmc1* null mutant allele (Figure 1B). This result is intriguing as it suggests that in the presence of DMC1 and in the absence of HOP2, RAD51-mediated repair is suppressed. Consistent with our data, we suggest a model (Figure 7) in which HOP2/MND1 is needed to overcome constraints imposed on RAD51-mediated repair in the presence of DMC1. These constraints may either be of mechanical nature or embedded in a signal pathway. In this sense, DMC1 may block access of RAD51 to ssDNA, while not being sufficiently activated for repair reactions in the absence of functional HOP2/MND1. Alternatively, HOP2/MND1 may be part of a signaling pathway in which DMC1-coated nucleoprotein filaments elicit a signal to (transiently) inhibit RAD51-mediated IS repair, which is only alleviated after DMC1-nucleoprotein filament interaction with HOP2. In both scenarios, HOP2/MND1 would be dispensable in the absence of DMC1 for RAD51-mediated IS repair. In the presence of DMC1, high levels of HOP2/MND1 would sufficiently activate DMC1 for meiotic DNA repair and, as shown before (Kurzbauer et al., 2012), RAD51 would only have a limited back-up function (Figure 7). This backup function is anticipated to be needed in case DMC1-coated nucleoprotein filaments fail to repair via the homologous chromosome (for example, because of sequence variation). We speculate that the inhibition of RAD51 has to be transient and eventually alleviated during progression of wild-type meiosis.

Such a negative regulatory mechanism suppressing RAD51 function during meiosis has not yet been described in plants, while in *S. cerevisiae*, several factors that indirectly promote IH bias by suppressing meiotic IS repair have been found. Suppression of IS repair is mediated by the activation of the Thr/Ser DNA damage checkpoint kinase Mek1 (for Meiosis-specific serine/threonine protein kinase1) in response to activated Red1 and Hop1, two structural components of the meiotic chromosome axis (Schwacha

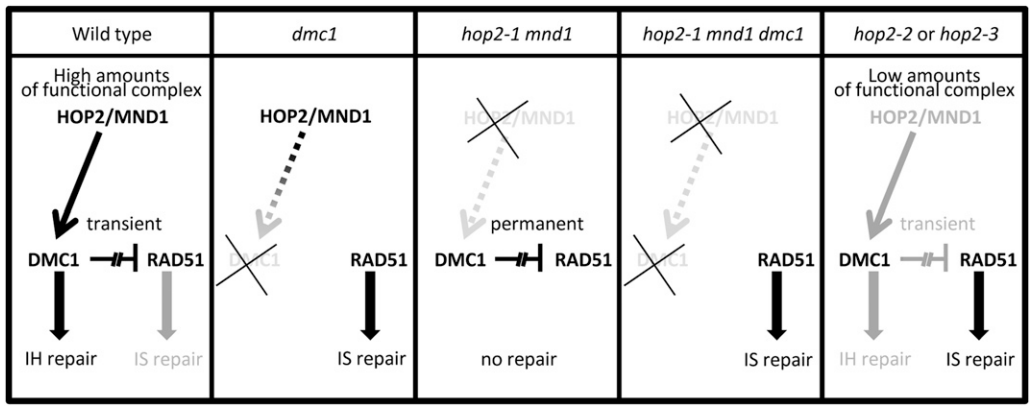

Figure 7. Model of the Functional Relationship between HOP2/MND1, DMC1, and RAD51.

In a wild-type context, high levels of HOP2/MND1 stimulate DMC1 activity, thereby promoting IH DNA repair. We anticipate that RAD51-mediated IS DNA repair is transiently repressed, limiting IS repair to a backup function. In the absence of DMC1, RAD51 efficiently repairs meiotic DSBs via sister chromatids. We anticipate that this repair is independent of HOP2/MND1, since in *hop2 mnd1 dmc1* triple mutants, IS DNA repair is in place. Importantly, in the absence of HOP2 and/or MND1, DMC1 is not stimulated and permanently inhibits RAD51-mediated IS DNA repair. Therefore, in the absence of HOP2/MND1, RAD51-mediated DNA repair can only take place if DMC1 is removed. Last, in conditions with only limited amounts of functional HOP2/MND1 complex available (*hop2-2* and *hop2-3* mutant alleles), DMC1 is not optimally supported and only limited IH DNA repair takes place. The limited stimulation of DMC1 is sufficient to indirectly promote RAD51-mediated IS repair. Possible mechanisms are discussed in the text.

and Kleckner, 1997; Wan et al., 2004; Niu et al., 2005). In brief, Mek1-mediated phosphorylation of Rad54, a protein promoting Rad51 function, (Niu et al., 2009), and binding of Hed1 to Rad51 (Tsubouchi and Roeder, 2006; Busygina et al., 2008) limit Rad51's repair function in the absence of Dmc1.

While no plant homologs of Mek1 or Hed1 are known yet, the HORMA domain (for Hop1p, Rev7p, Mad2) protein ASY1 is conserved among plant species and shares homology with Hop1 from yeast (de los Santos and Hollingsworth, 1999). *Arabidopsis* mutants lacking *ASY1* preferentially repair meiotic DSBs via the sister chromatids (Sanchez-Moran et al., 2007). Even though a protein related to yeast's Red1, ASY3, has recently been described in *Arabidopsis* (Ferdous et al., 2012), genetic evidence and the lack of a clear Mek1 homolog suggest that IH repair in plants is rather directly promoted via ASY1, HOP2, MND1, and DMC1 and not indirectly by suppression of RAD51-mediated IS repair. Recent data demonstrated that plant DMC1 is a promiscuous recombinase, proficient at repair from either the sister or the homolog, and its IH specificity is mediated by factors like ASY1 (Sanchez-Moran et al., 2007; Kurzbauer et al., 2012).

DMC1-Driven IH Repair Is Dependent on the Level of Functional HOP2/MND1

The most prominent feature of the hypomorphic *hop2-2* and *hop2-3* mutants is their deficiency in IH bias, while retaining their capacity for IS DNA repair (Figure 1). This is in clear contrast with the observations made in the *hop2-1* null allele (Schommer et al., 2003; Stronghill et al., 2010), which exhibits impaired meiotic DNA repair. Genetic crosses revealed that the IS repair observed in the hypomorphic *hop2-2* and *hop2-3* alleles depends on the presence of RAD51, MND1, but not on DMC1. It therefore appears that in the presence of either low amounts (*hop2-2*) or less stable (*hop2-3*) HOP2/MND1 complex, DMC1 is not sufficiently activated to promote IH repair but is sufficiently activated to allow IS DNA repair, potentially mediated via RAD51. It is important to note that RAD51-mediated IS repair does not directly depend on HOP2/MND1, since a *hop2-1 mnd1 dmc1* triple mutant appears like a *dmc1* single mutant in which DSBs are formed but repaired in a RAD51-dependent manner via the sister chromatid.

The Plant HOP2/MND1 Complex Binds to DNA and Stimulates DMC1-Mediated D-Loop Formation

We further performed a systematic analysis of DNA binding characteristics of HOP2 and MND1. We found that both proteins, HOP2 and MND1, are important for ssDNA and dsDNA binding in vitro. In more detail, we could show that the N termini of both HOP2 and MND1 are important for binding DNA in vitro, supporting the idea that they cooperate to form a DNA binding platform. It is interesting to note that both the N-terminal domains of HOP2 and MND1 are rich in conserved Lys and Arg residues, which are thought to be involved in DNA binding. We substituted all conserved Lys residues in the N-terminal domain of HOP2 from *Arabidopsis* individually with Ala (Lys21Ala, Lys39Ala, Lys44Ala, Lys58Ala, and Lys62Ala) and observed that only the substitution Lys58Ala exhibits a prominent effect on DNA binding in the HOP2/MND1 complex of *Arabidopsis*. Individual Lys-to-Ala (Lys30Ala, Lys34Ala, Lys47Ala, and Lys63Ala) substitutions of residues in the N-terminal domain of MND1 had no impact on DNA binding, indicating that only substitutions of multiple residues may have an impact on DNA binding, as also shown recently for mouse HOP2/MND1 (Zhao et al., 2013).

The performed D-loop assay clearly demonstrates that in plants, the HOP2/MND1 complex also stimulates DMC1, as has been shown earlier for heterologously expressed and purified proteins from human, mouse, and budding yeast, and the extent of DMC1 stimulation is also comparable (Chen et al., 2004; Petukhova et al., 2005; Enomoto et al., 2006). It is interesting to note that Os-DMC1A has higher basic activity but is less responsive to the addition of Os-HOP2/Os-MND1 (twofold stimulation), while Os-DMC1B has very low D-loop activity that can strongly be activated by the addition of Os-HOP2/Os-MND1 (14-fold). Importantly, our experiments also demonstrate that the plant HOP2/MND1 complex has no intrinsic D-loop-forming activity (Figure 6).

Taken together, the results outlined above provide explanations for the observed phenotypes in *hop2-2* and *hop2-3* mutant plants. Plant HOP2/MND1 is a crucial cofactor of DMC1-mediated D-loop formation and, therefore, of DNA repair in meiosis. Our analysis revealed negative regulation of RAD51 by DMC1 during meiosis. We believe that this negative regulation is of a transient nature and is important for the establishment of DMC1-mediated interhomolog connections during meiotic DNA repair. Reduced availability of functional HOP2/MND1 complex leads to suboptimal support of DMC1 and, therefore, to a failure to repair meiotic DSBs via the homologous chromosome but is sufficient to allow RAD51-mediated IS repair.

METHODS

Plant Material

Arabidopsis thaliana wild-type plant material used in this study is Wassilewskija-4 (Ws-4) or L*er*. The *hop2-1* (*ahp2-1*) mutant line is in the L*er* ecotype and has been described previously (Schommer et al., 2003). *hop2-2* and *hop2-3* mutant lines were obtained from the Versailles collection (Ws-4 accession; http://www-ijpb.versailles.inra.fr/en/sgap/equipes/fichiers.old-christine/T-DNA_information.htm). (Bechtold et al., 1993; De Muyt et al., 2009). All other mutant lines were described earlier: *asy1-3* (Institut National de la Recherche Agronomique line EJZ8, Ws-4 ecotype; De Muyt et al., 2009), *mre11-3* (SALK_054418, Columbia ecotype; Puizina et al., 2004), *mnd1-1* (SALK_110052, Columbia ecotype; Kerzendorfer et al., 2006), *rad51-1* (Columbia ecotype; Li et al., 2004), and *dmc1-1* (Wassilewskija [Ws] ecotype; Couteau et al., 1999; Li et al., 2004).

Growth Conditions

Arabidopsis plants were cultivated in a greenhouse or growth chambers under the following conditions: photoperiod 16 h/day and 8 h/night; temperature 20°C day and night; humidity 70%.

Genetic Analyses

Allelism tests were performed by crossing plants heterozygous for each mutation. Heteroallelic plants were identified by PCR using specific primers (see below). Double mutants were obtained by crossing plants heterozygous for each mutation. The resulting hybrids were obtained after self-pollination. PCR screening was then used to identify plants homozygous for both mutations in the F2 progeny.

Genotyping

The *hop2-1* and *hop2-2* mutants have been described earlier (Schommer et al., 2003; De Muyt et al., 2009). In case of *hop2-3* mutant alleles, the altered genomic regions at the *HOP2* gene locus were PCR amplified using specific primer sets. Amplification products obtained from sterile plants were analyzed initially by gel electrophoresis and sequencing, as previously described (De Muyt et al., 2009), and subsequently by gel electrophoresis only.

To determine the genotype in *hop2-1* mutant plants by PCR, the primer-set AHP2_P7 (5′-GAAAACTATCAGTGATGTGG-3′) and AHP2_B (5′-CCTCGAGGCCTCTTTTTACC-3′) was used to amplify the wild-type sequence (632 bp) and primer set AHP2_P7 and GABIo8409 (5′-ATATTGACCAT-CATACTCATTGC-3′) to amplify a 572-bp fragment present in *hop2-1* mutant plants. The deletion present in *hop2-2* mutants was determined by PCR using the primer set N6360002U (5′-CACCATCAATACAAAAGACG-3′) and N6360002L (5′-CCAAGTGATTAAATTCCCAG-3′), yielding a fragment of 900 bp in case of presence of the wild-type allele and of 750 bp in case of presence of the *hop2-2* mutant allele. The deletion found in *hop2-3* mutants was determined by PCR using the primers set AHP2_P7 and Hop2-1L (5′-TTGTACAGTTGCATATGTGTG-3′) to amplify a 700-bp fragment in case of the presence of the wild-type allele and a 572-bp fragment in case of presence of the *hop2-3* mutant allele.

cDNA Characterization

For RT-PCR experiments, mRNA was obtained from flower buds, roots, or leaf tissues as described (De Muyt et al., 2007) and reverse transcribed into cDNA, and the amounts were normalized to the expression of the adenine phosphoribosyltransferase-encoding gene (*APT*; Moffat et al. 1994) using primers APT_RT1 (5′-TCCCAGAATCGCTAAGATTGCC-3′) and APT_RT2-1 (5′-CTCAATTACGCAAGCAC-3′) for 30 PCR cycles (annealing temperature of 60°C).

The *HOP2* CDS was amplified using different sets of primers: AHP2_C (5′-TGATTTCTGATTCCACATCACTG-3′) and AHP2_D (5′-AAATCGGA-TAACACCGAAGC-3′), AHP2_7 (5′-GAAAACTATCAGTGATGTGG-3′) and AHP2_B (5′-CCTCGAGGCCTCTTTTTACC-3′), or AHP2_A (5′-GGTGAGGCCAGAAGACAAAA-3′) and AHP2_B for 35 cycles (annealing temperature of 60°C).

For *hop2-3*, the internal deletion was determined using primers AHP2_P7 and AHP2_B, yielding a 384-bp fragment in wild-type plants and a 342-bp fragment for mRNA coming from *hop2-3* mutant plants. The RT-PCR products were cloned into vector Zero Blunt (Invitrogen) and sequenced by LGC Genomics (see Supplemental Figure 2 online).

Quantitative RT-PCR

Total RNA from *hop2-2* and wild-type (Ws-4) *Arabidopsis* flower buds from several different individual plants was extracted using the SV Total RNA isolation system (Promega) according to the manufacturer's instructions. Subsequently, cDNA was synthesized using the iScript cDNA synthesis kit (Bio-Rad) and quantitative PCR was performed with a Bio-Rad iQ5 Cycler using the iQ SYBR green supermix and the following program: step 1, 95°C, 3 min; step 2, 95°C, 15 s; step 3, 60°C, 30 s; step 4, 72°C, 30 s; repeat steps 2 to 4 50 times; step 5, 94°C, 1 min; step 6, 60°C, 1 min; step 7, 60°C, 30 s with increasing the temperature over 71 cycles (0.5°C/cycle, end temperature 95°C). Primers for the amplicon adjacent to the ATG were HOP2_5′ATG_fw (5′-TGCTCTCGCTTCAGGTTTTT-3′) and HOP2_5′ATG_rv (5′-CGAAA-TAATTGGCGGGAAAT-3′) and for the amplicon bridging exons 4 and 5 were HOP2_3′hop2-1_fw (5′-AAGAGAAAGATGCCAAACTAAGG-3′) and HOP2_3′hop2-1_rv (5′-AGTTTCTCTTCCATTTCCTTAAC-3′). Two technical repeats were performed. All values were normalized to *Actin2/7* gene expression using primers actin_ampl3_dn (5′-TTGCTGACCGTATGAGCAAA-GA-3′) and actin_ampl3_up (5′-TCGATGGACCTGACTCATCGT-3′). mRNA quality, lack of contaminating genomic DNA, and concentration were determined prior to each experiment. Additionally, melting point analysis was performed with each amplicon. Data analysis and calculation of expression profiles were performed with iQ5 optical system software.

Antibodies

Primary antibodies for fluorescent immunolocalization of proteins were used as follows: αASY1 raised in rabbit (1:500 diluted in blocking buffer; PBS + 0.1% Triton + 3% BSA) (Armstrong et al., 2002), αASY1 raised in rat (1:500; Higgins et al., 2004), αMND1 raised in rat (1:200; Vignard et al., 2007), αRAD51 raised in rat (1:500; Kurzbauer et al., 2012), and αDMC1 raised in rabbit (1:20; Chelysheva et al., 2007). Secondary antibodies were used as follows: goat-anti-rabbit conjugated to fluorescein isothiocyanate (1:300; Sigma-Aldrich), goat-anti-rat conjugated to Cy3 (1:300; Chemicon), goat-anti-rabbit conjugated to Alexa 488 (1:100; Invitrogen), goat-anti-rat conjugated to Alexa 488 (1:100; Invitrogen), and goat-anti-rat conjugated to Alexa 568 (1:100; Invitrogen).

Microscopy

Comparison of early stages of microsporogenesis and the development of pollen mother cells was performed as described (Grelon et al., 2001). Preparation of prophase stage spreads for immunocytology was performed according to Armstrong et al. (2002) with the modifications described (Chelysheva et al., 2005, 2010; Kurzbauer et al., 2012).

Parts of the observations were made using a Leica DM RXA2 microscope or a Zeiss Axio Imager 2 microscope; photographs were taken using a CoolSNAP HQ camera (Roper Scientific) driven by OpenLAB 4.0.4 software or a Zeiss camera AxioCam MR driven by Axiovision 4.7. All of the images acquired were further processed with OpenLAB 4.0.4, Axiovision 4.7, or AdobePhotoshop 7.0 (Adobe). Other parts of the analysis were performed on a Zeiss Axioplan microscope, where Z-stacks with 100-nm intervals were acquired with MetaMorph software. Z-stacks were deconvolved using AutoQuant software and are presented as projections done with HeliconFocus software. Recombinase foci were counted manually with the help of the "count" tool in Adobe Photoshop CS4.

Generation of Protein Expression Constructs for Heterologous Expression in *Escherichia coli*

In order to coexpress *Arabidopsis* HOP2 and MND1 in *E. coli*, the CDSs of both HOP2 and MND1 were cloned into the vector pRSFDuet-1 (Merck). First, the CDS of MND1 (Kerzendorfer et al., 2006) was amplified by PCR using KOD DNA polymerase (Merck) and the primer pair MND_FWD_duet (5′-TATCATATGTCTAAGAAACGGGGAC-3′) and MND_REV_duet (5′-ATACTCGAGCTAAGCTTCATCTTGTACT-3′). Each primer included either an *Nde*I or an *Xho*I restriction site, which were later used to clone MND1 in frame into the second multiple cloning site (MCS) of the plasmid pRSFDuet-1. Second, the CDS of HOP2 (Schommer et al., 2003) was amplified by PCR using *Thermococcus kodakaraensis* KOD1 DNA Polymerase and the primer pair AHP2_FWD_duet (5′-AACGGATCC-TATGGCTCCTAAATCGGATAACAC-3′) and AHP2_REV_duet (5′-ATA-CTGCAGTTACTGTCCTCGAGGCCTC-3′). Each primer included either a *Bam*HI or a *Pst*I restriction site, which were later used to insert HOP2 in frame into the first MCS of the plasmid pRSFDuet-1/MND1. As a result, the recombinant HOP2 protein is expressed with an N-terminal 6xHIS-tag and the MND1 protein is expressed without any additional amino acids from the vector pRSFDuet-1/HOP2/MND1.

To construct the expression plasmid for the N-terminal truncated version of the recombinant HOP2 protein (Met84-Gln226), the primer pair AHP2-84Met-fwd (5′-AGGATCCTATGAAAGAAGACAATGCCAAAC-3′) and AHP2_REV_duet (5′-ATACTGCAGTTACTGTCCTCGAGGCCTC-3′) was used for PCR (KOD DNA polymerase) and pRSFDuet-1/HOP2/MND1

as a template. Each primer included either a *Bam*HI or a *Pst*I restriction site, which were later used to clone the sequence of ΔN-HOP2 in frame into the first MCS of the plasmid pRSFDuet-1/MND1.

The small deletion (Glu-123–Glu-136) in the HOP2 sequence that corresponds to the *hop2-3* hypermorphic allele was generated by deletion PCR. To this end, the outlined above vector pRSFDuet-1/HOP2/MND1 was used as a template for PCR amplification using KOD DNA polymerase with a forward primer that was phosphorylated at the 5′ end (Phos/5′-AAGAGAAACTGGTCAAACTAC-3′) and a reverse primer (5′-GTATCT-CTTCTAGTGTCAAGT-3′). These two primers were designed to anneal exactly to the border sequences adjacent but outside of the deletion in the *hop2-3* hypomorphic allele with their 3′ ends pointing away from the deletion. After amplification, the PCR product was gel purified and ligated with T4 DNA ligase in green buffer (Fermentas). Subsequently the ligase was heat inactivated at 70°C for 20', and the restriction enzyme *Dpn*I was added to the reaction mixture for 2 h at 37°C. Finally, the solution was transformed into chemical competent XL-1 Blue *E. coli* cells, and the success of the deletion PCR was verified by restriction analysis using *Dra*I together with *Eco*RI and subsequent sequencing. All PCR products were confirmed by sequencing. Further information on truncated HOP2 and MND1 protein variants can be found in Supplemental Methods 1 online. All primers employed to construct the various truncated versions are compiled in Supplemental Table 1 online.

In order to coexpress rice (*Oryza sativa* spp *japonica*) HOP2 and MND1 in *E. coli*, the protein CDSs of both were synthesized (see Supplemental Table 2 online for sequence details) (GeneArt, Invitrogen) and subsequently cloned into the vector pRSFDuet-1 (Merck) using the *Bam*HI and *Xho*I restriction sites. As a result, recombinant Os-HOP2 protein is expressed with an N-terminal 6xHis-tag and the Os-MND1 protein is expressed without any additional amino acids from the vector pRSFDuet-1/OsHOP2/OsMND1.

The small deletion (Ser-123–Glu-136) in the Os-HOP2 sequence, corresponding to the *Arabidopsis hop2-3* hypomorphic allele, was generated by deletion PCR (see Supplemental Table 3 online for multiple protein sequence alignment of At-HOP2, At-HOP2-3, and Os-HOP2). To this end, the vector pRSFDuet-1/OsHOP2/OsMND1 served as a template in PCR amplification (Phusion high-fidelity DNA polymerase; New England Biolabs,) with a phosphorylated forward primer (Phos/5′-GAGAAACTGAATAAACTGCGC-3′) and a nonmodified reverse primer (5′-TTTGATTTCTGCCAGGGTCAG-3′). These two primers were designed to anneal exactly to the border sequences adjacent but outside of the deletion with their 3′ ends pointing away from the deletion. After amplification, the PCR product was gel purified and ligated (T4 DNA ligase; Fermentas). Subsequently, the ligase was heat inactivated at 70°C for 20' and the restriction enzyme *Dpn*I was added to the reaction mixture for 2 h at 37°C. Finally, the solution was transformed into chemical competent XL-1 Blue *E. coli* cells and the obtained plasmid verified by sequencing.

Expression and Purification of Recombinant Proteins from *E. coli*

The plasmids for expression of the protein complexes (from *Arabidopsis* and rice) HOP2/MND1 as well as the truncated versions ΔN-HOP2/MND1 and HOP2-3/MND1 were transformed into chemically competent Rosetta (DE3)pLysS *E. coli* cells (Merck), and expression was started by auto-induction (Studier, 2005). To this end, a single colony was inoculated in 3 mL of ZYP-0.8G liquid medium [1 mM $MgSO_4$, 0.05 M KH_2PO_4, 0.05 M Na_2HPO_4, 0.025 M $(NH_4)_2SO_4$, 1% peptone, 0.5% yeast extract, 0.8% Glc, and 0.01% kanamycin], and after several hours of incubation at 37°C with 200 rpm, 1 mL was added to two liters of ZYP-5052 liquid medium [1 mM $MgSO_4$, 0.05 M KH_2PO_4, 0.05 M Na_2HPO_4, 0.025 M $(NH_4)_2SO_4$, 1% peptone, 0.5% yeast extract, 0.5% glycerol, 0.05% Glc, 0.2% lactose, and 0.01% kanamycin]. On the next day, the cells were harvested by centrifugation (5000*g*, 30', 4°C). The cell pellet was frozen at −20°C and thawed on ice. Subsequent resuspension of the pellet in ice cold buffer A (1 g pellet per 5 mL of 50 mM phosphate buffer, pH 8.0, with 500 mM NaCl, 2 mM β-mercaptoethanol, 0.05% Nonidet P-40, and one tablet of Complete-Mini EDTA-free [Roche] per 50 mL of buffer) was followed by sonication on ice. After that, an additional centrifugation (20,000*g*, 30', 4°C) was conducted, and the resulting precleared lysate was incubated with 5 mL of Ni-beads (Profinity IMAC Ni-charged resin; Bio-Rad) for 1 h at 4°C. The Ni-beads were washed four times with buffer A, and the recombinant 6xHis-tagged proteins were eluted with 1 M imidazole, pH 8.0, in buffer A. After elution, the protein solution was concentrated with the help of Vivaspin 20 10,000 MWCO polyethersulfone membrane centrifugal concentrators (Sartorius Stedim Biotech), and gel filtration was performed using an ÄKTA fast protein liquid chromatography system, a Superdex 200 16/60 column (GE Healthcare Life Sciences), and buffer A. The fractions that contained the protein complex were pooled and aliquots were shock frozen in liquid nitrogen and stored at −80°C. The purity and concentration of the recombinant proteins was analyzed by SDS-PAGE using Coomassie Brilliant Blue staining and Bradford assay according to standard techniques. Finally, the identities of the Coomassie Brilliant Blue–stained bands for the HOP2/MND1 complex were confirmed by mass spectrometry (see Supplemental Table 4 online). Information on At-DMC1 protein expression in Hi-5 insect cells can be found in the Supplemental Methods 1 and in Supplemental Table 5 online.

EMSA

Affinity-purified HOP2/MND1, ΔN-HOP2/MND1, HOP2-3/MND1, and HOP2/MND1 protein complex variants (protein concentrations are denoted in the figures) were incubated with circular ssDNA ΦX174 virion (20 μM/bp; NEB) and/or linearized dsDNA ΦX174 Replication form I (20 μM/bp; NEB) for 10' at room temperature. Subsequently, the DNA-protein complex was mixed with 6× Luria-Bertani (15% Ficoll-400, 50 mM EDTA, pH 8, and 0.15% Orange G), separated on a 0.8% agarose gel (1× TAE: 40 mM Tris, 20 mM acetic acid, and 1 mM EDTA, pH 8) at 4°C, and visualized by staining with ethidium bromide.

Temperature-Mediated Unfolding Followed by ECD Spectroscopy

Thermal unfolding was followed by ECD spectroscopy (Chirascan, Applied Photophysics). The instrument was flushed with nitrogen at a flow rate of 5 liters min^{-1} and was equipped with a Peltier element for temperature control. Temperature-mediated denaturation was monitored between 20 and 85°C. The temperature was increased stepwise at 1.0°C min^{-1}. Single-wavelength scans were performed with instrumental parameters set as follows: for far-UV ECD at 222 nm, 5 μM HOP2/MND1 or HOP2-3/MND1 in 5 mM phosphate buffer, pH 7.7; path length, 1 mm; spectral bandwidth, 3 nm; scan time per point, 10 s. ECD spectra in the far-UV region (190 to 280 nm) were recorded for 5 μM HOP2/MND1 and 5 μM HOP2-3/MND1 at 20°C, at 85°C after thermal unfolding, and at 20°C again after heating and cooling. The fraction α of unfolded protein was calculated according to $\alpha = (\theta N - \theta)/(\theta N - \theta U)$ with θN being the ellipticity (in mdeg) at 222 nm of the protein in the native folded state, θ the ellipticity at defined temperature (T), and θU being the ellipticity at 222 nm of the completely unfolded state.

D-Loop Assay

DNA Substrates

For the D-loop formation assay, HPLC-purified DNA oligonucleotides were purchased from Nihon Gene Research Laboratory: G5E4 90mer, 5′-CCTGCCTAGGCAAAATAGCACCCTCCCGCTCCAGAACAACATACA-GCGCTTCCACAGCGGCAGCCATAACAGTCAGCCTTACCAGTAAAA-3′. The superhelical dsDNAs were prepared as described (Kagawa et al., 2001). To prevent the superhelical dsDNA from undergoing irreversible denaturation, alkaline treatment of the cells harboring the plasmid DNA was avoided.

D-Loop Formation Assay

Os-DMC1A or Os-DMC1B (Sakane et al., 2008) (400 nM) was incubated with the ^{32}P-labeled G5E4 90-mer single-stranded oligonucleotide (1 μM) at 37°C for 5 min, in 8 μL of reaction buffer, containing 22 mM HEPES, pH 7.5, 50 mM KCl, 0.025 mM EDTA, 1 mM DTT, 0.2 mM 2-mercaptoethanol, 1% glycerol, 1 mM $MgCl_2$, 1 mM ATP, 20 mM creatine phosphate, 75 μg/mL creatine kinase, and 100 μg/mL BSA. After this incubation, 1 μL of rice HOP2/MND1 or HOP2-3/MND1 was added, and the samples were further incubated at 37°C for 5 min. The HOP2/OsMND1 or HOP2-3/MND1 concentrations were 12.5, 25, and 50 nM. Subsequently, 1 μL of the CP943 superhelical dsDNA (30 μM) was added, and the reactions were continued at 37°C for 10 min. The reactions were terminated by the addition of 2 μL of stop solution containing SDS (0.2%) and proteinase K (1.4 mg/mL; Roche Applied Science), and the deproteinized DNA products were separated by 1% agarose gel electrophoresis in 1× TAE buffer at 4 V/cm for 2 h. The gels were dried and exposed to an imaging plate. The gel images were visualized using an FLA-7000 imaging analyzer (Fujifilm), and the band intensities were quantitated with Multi Gauge software (Fujifilm).

Accession Numbers

Sequence data for the genes from this article can be found in the GenBank/EMBL data libraries under the following accession numbers: AT1G13330 (At-*HOP2*), AT4G29170 (At-*MND1*), AT5G20850 (At-*RAD51*), AT3G22880 (At-*DMC1*), AT1G67370 (At-*ASY1*), AT5G54260 (At-*MRE11*), Os12g0143800 (Os-*DMC1A*), Os11g0146800 (Os-*DMC1B*), Os09g0280600 (Os-*MND1*), Os03g0710100 (Os-*HOP2*). Sequence data for the proteins from this article are as follows: Q9FX64 (Swiss-Prot) (At-HOP2), CAJ44238 (EMBL) (At-MND1), AAC49617 (GenBank) (At-DMC1), ABF98498 (GenBank) (Os-HOP2), BAF24680 (DDBJ) (Os-MND1), AAM76791 (GenBank) (Os-DMC1A), and AAM76792 (GenBank) (Os-DMC1B).

Supplemental Data

The following materials are available in the online version of this article.

Supplemental Figure 1. Epistasis Analysis.

Supplemental Figure 2. Molecular Characterization of *hop2-2* and *hop2-3* Alleles.

Supplemental Figure 3. DSBs Are Formed in the *hop2-2* and *hop2-3* Mutants.

Supplemental Figure 4. No Major Differences in DMC1 and RAD51 Foci Numbers Are Observed among All *hop2* Mutant Alleles.

Supplemental Figure 5. HOP2 and HOP2-3 Form Protein Complexes with MND1.

Supplemental Figure 6. Putative Coiled Coil Domains of Both HOP2 and MND1 Are Sufficient for Complex Formation.

Supplemental Figure 7. The N-Terminal Domains of Both MND1 and HOP2 Are Needed for DNA Binding of the HOP2/MND1 Protein Complex.

Supplemental Figure 8. The N-Terminal Domain of HOP2 Is Not Sufficient for DNA Binding.

Supplemental Figure 9. The HOP2/MND1 Complex Is More Proficient at DNA Binding Than HOP2 Alone.

Supplemental Figure 10. The HOP2/MND1 protein complex is heterodimeric

Supplemental Figure 11. The Recombinase DMC1 Binds to Wild-Type HOP2/MND1 and the Variant ΔN-HOP2/MND1 and HOP2-3/MND1 Protein Complexes in Vitro.

Supplemental Table 1. Primer Sequences for Construction of Truncated HOP2/MND1 Complexes.

Supplemental Table 2. Sequence of Rice HOP2/MND1 Synthesized by Geneart.

Supplemental Table 3. Multiple Sequence Alignment of *Arabidopsis* HOP2 and HOP2-3 and Rice HOP2.

Supplemental Table 4. Mass Spectrometric Determination of the Protein Identity of Heterologously Expressed At-HOP2 and At-MND1 Proteins.

Supplemental Table 5. Codon-Optimized At-*DMC1* Sequence for Expression in Hi5 Insect Cells

Supplemental Methods 1. Description of Experimental Procedures Related to Supplemental Data.

Supplemental References 1. References Related to Experimental Procedures Described in Supplemental Methods 1.

ACKNOWLEDGMENTS

We thank Stefan Hofbauer from the Obinger Lab at the University of Natural Resources and Life Sciences (Vienna, Austria) for technical assistance with ECD. We also thank Dorothea Anrather (Max F. Perutz Laboratories, University of Vienna, Austria) for mass spectrometry analysis of the recombinant protein complex HOP2/MND1, Peggy Stolt-Bergner (Campus Support Facility, Vienna, Austria) for expression of the DMC1 in Hi5 insect cells, and Aurélie Chambon (Institut Jean-Pierre Bourgin) for technical assistance. We thank Pascale Doutriaux (Université Paris-Sud 11, Orsay, France) for generously supplying the At-*DMC1* cDNAs. We thank the European Union (FP7 program Meiosys-KBBE-2009-222883), Institut National de la Recherche Agronomique (Department of Biologie et Amélioration des Plantes), Agence Nationale pour la Recherche (ANR07-BLAN-0215), and Rijk Zwaan for funding our research.

AUTHOR CONTRIBUTIONS

C.U., A.R., and M.V.H. performed most of the experiments, evaluated the data, and wrote parts of the article. C.U. performed all biochemical experiments (apart from Os-DMC1A/B purification and the D-loop assay). M.V.H. performed parts of the cytology and the molecular characterization. A.R. performed parts of the cytology and the molecular characterization. A.D.M. and D.V. were involved in the initial screen and mutant mapping. L.P. performed some of the experiments for the molecular characterization. L.C. performed some of the cytological characterization. W.K. and H.K. purified OsDMC1A/B and performed the D-loop assay. P.S. and M.G. designed the experiments, evaluated the data, and wrote the article.

Received September 25, 2013; revised November 24, 2013; accepted December 5, 2013; published December 20, 2013.

REFERENCES

Allers, T., and Lichten, M. (2001). Differential timing and control of noncrossover and crossover recombination during meiosis. Cell **106:** 47–57.

Armstrong, S.J., Caryl, A.P., Jones, G.H., and Franklin, F.C. (2002). Asy1, a protein required for meiotic chromosome synapsis, localizes to axis-associated chromatin in *Arabidopsis* and Brassica. J. Cell Sci. **115:** 3645–3655.

Baudat, F., and de Massy, B. (2007). Regulating double-stranded DNA break repair towards crossover or non-crossover during mammalian meiosis. Chromosome Res. **15:** 565–577.

Baumann, P., Benson, F.E., and West, S.C. (1996). Human Rad51 protein promotes ATP-dependent homologous pairing and strand transfer reactions in vitro. Cell **87:** 757–766.

Bechtold, N., Ellis, J., and Pelletier, G. (1993). In planta Agrobacterium-mediated gene transfer by infiltration of adult *Arabidopsis thaliana* plants. Comptes Rendus Acad. Sci. Ser. Iii-Sciences De La Vie. Life Sciences. **316:** 1194–1199.

Benson, F.E., Stasiak, A., and West, S.C. (1994). Purification and characterization of the human Rad51 protein, an analogue of *E. coli* RecA. EMBO J. **13:** 5764–5771.

Bergerat, A., de Massy, B., Gadelle, D., Varoutas, P.C., Nicolas, A., and Forterre, P. (1997). An atypical topoisomerase II from Archaea with implications for meiotic recombination. Nature **386:** 414–417.

Bishop, D.K. (1994). RecA homologs Dmc1 and Rad51 interact to form multiple nuclear complexes prior to meiotic chromosome synapsis. Cell **79:** 1081–1092.

Bishop, D.K., Park, D., Xu, L., and Kleckner, N. (1992). DMC1: A meiosis-specific yeast homolog of *E. coli* recA required for recombination, synaptonemal complex formation, and cell cycle progression. Cell **69:** 439–456.

Bishop, D.K., and Zickler, D. (2004). Early decision; meiotic crossover interference prior to stable strand exchange and synapsis. Cell **117:** 9–15.

Busygina, V., Sehorn, M.G., Shi, I.Y., Tsubouchi, H., Roeder, G.S., and Sung, P. (2008). Hed1 regulates Rad51-mediated recombination via a novel mechanism. Genes Dev. **22:** 786–795.

Callender, T.L., and Hollingsworth, N.M. (2010). Mek1 suppression of meiotic double-strand break repair is specific to sister chromatids, chromosome autonomous and independent of Rec8 cohesin complexes. Genetics **185:** 771–782.

Cao, L., Alani, E., and Kleckner, N. (1990). A pathway for generation and processing of double-strand breaks during meiotic recombination in *S. cerevisiae*. Cell **61:** 1089–1101.

Chelysheva, L., et al. (2005). AtREC8 and AtSCC3 are essential to the monopolar orientation of the kinetochores during meiosis. J. Cell Sci. **118:** 4621–4632.

Chelysheva, L., Gendrot, G., Vezon, D., Doutriaux, M.P., Mercier, R., and Grelon, M. (2007). Zip4/Spo22 is required for class I CO formation but not for synapsis completion in *Arabidopsis thaliana*. PLoS Genet. **3:** e83.

Chelysheva, L., Grandont, L., Vrielynck, N., le Guin, S., Mercier, R., and Grelon, M. (2010). An easy protocol for studying chromatin and recombination protein dynamics during *Arabidopsis thaliana* meiosis: Immunodetection of cohesins, histones and MLH1. Cytogenet. Genome Res. **129:** 143–153.

Chen, Y.K., et al. (2004). Heterodimeric complexes of Hop2 and Mnd1 function with Dmc1 to promote meiotic homolog juxtaposition and strand assimilation. Proc. Natl. Acad. Sci. USA **101:** 10572–10577.

Cloud, V., Chan, Y.L., Grubb, J., Budke, B., and Bishop, D.K. (2012). Rad51 is an accessory factor for Dmc1-mediated joint molecule formation during meiosis. Science **337:** 1222–1225.

Couteau, F., Belzile, F., Horlow, C., Grandjean, O., Vezon, D., and Doutriaux, M.P. (1999). Random chromosome segregation without meiotic arrest in both male and female meiocytes of a dmc1 mutant of *Arabidopsis*. Plant Cell **11:** 1623–1634.

de los Santos, T., and Hollingsworth, N.M. (1999). Red1p, a MEK1-dependent phosphoprotein that physically interacts with Hop1p during meiosis in yeast. J. Biol. Chem. **274:** 1783–1790.

De Massy, B., Baudat, F., and Nicolas, A. (1994). Initiation of recombination in *Saccharomyces cerevisiae* haploid meiosis. Proc. Natl. Acad. Sci. USA **91:** 11929–11933.

De Muyt, A., Pereira, L., Vezon, D., Chelysheva, L., Gendrot, G., Chambon, A., Lainé-Choinard, S., Pelletier, G., Mercier, R., Nogué, F., and Grelon, M. (2009). A high throughput genetic screen identifies new early meiotic recombination functions in *Arabidopsis thaliana*. PLoS Genet. **5:** e1000654.

De Muyt, A., Vezon, D., Gendrot, G., Gallois, J.L., Stevens, R., and Grelon, M. (2007). AtPRD1 is required for meiotic double strand break formation in *Arabidopsis thaliana*. EMBO J. **26:** 4126–4137.

Dray, E., Dunlop, M.H., Kauppi, L., San Filippo, J., Wiese, C., Tsai, M.S., Begovic, S., Schild, D., Jasin, M., Keeney, S., and Sung, P. (2011). Molecular basis for enhancement of the meiotic DMC1 recombinase by RAD51 associated protein 1 (RAD51AP1). Proc. Natl. Acad. Sci. USA **108:** 3560–3565.

Dresser, M.E., Ewing, D.J., Conrad, M.N., Dominguez, A.M., Barstead, R., Jiang, H., and Kodadek, T. (1997). DMC1 functions in a *Saccharomyces cerevisiae* meiotic pathway that is largely independent of the RAD51 pathway. Genetics **147:** 533–544.

Edlinger, B., and Schlögelhofer, P. (2011). Have a break: Determinants of meiotic DNA double strand break (DSB) formation and processing in plants. J. Exp. Bot. **62:** 1545–1563.

Enomoto, R., Kinebuchi, T., Sato, M., Yagi, H., Kurumizaka, H., and Yokoyama, S. (2006). Stimulation of DNA strand exchange by the human TBPIP/Hop2-Mnd1 complex. J. Biol. Chem. **281:** 5575–5581.

Ferdous, M., Higgins, J.D., Osman, K., Lambing, C., Roitinger, E., Mechtler, K., Armstrong, S.J., Perry, R., Pradillo, M., Cuñado, N., and Franklin, F.C. (2012). Inter-homolog crossing-over and synapsis in *Arabidopsis* meiosis are dependent on the chromosome axis protein AtASY3. PLoS Genet. **8:** e1002507.

Garcia, V., Phelps, S.E., Gray, S., and Neale, M.J. (2011). Bidirectional resection of DNA double-strand breaks by Mre11 and Exo1. Nature **479:** 241–244.

Gasior, S.L., Olivares, H., Ear, U., Hari, D.M., Weichselbaum, R.R., and Bishop, D.K. (2001). Assembly of RecA-like recombinases: distinct roles for mediator proteins in mitosis and meiosis. Proc. Natl. Acad. Sci. USA **98:** 8411–8418.

Gerton, J.L., and DeRisi, J.L. (2002). Mnd1p: An evolutionarily conserved protein required for meiotic recombination. Proc. Natl. Acad. Sci. USA **99:** 6895–6900.

Goldfarb, T., and Lichten, M. (2010). Frequent and efficient use of the sister chromatid for DNA double-strand break repair during budding yeast meiosis. PLoS Biol. **8:** e1000520.

Greenfield, N.J. (2006). Using circular dichroism collected as a function of temperature to determine the thermodynamics of protein unfolding and binding interactions. Nat. Protoc. **1:** 2527–2535.

Grelon, M., Vezon, D., Gendrot, G., and Pelletier, G. (2001). AtSPO11-1 is necessary for efficient meiotic recombination in plants. EMBO J. **20:** 589–600.

Haaf, T., Golub, E.I., Reddy, G., Radding, C.M., and Ward, D.C. (1995). Nuclear foci of mammalian Rad51 recombination protein in somatic cells after DNA damage and its localization in synaptonemal complexes. Proc. Natl. Acad. Sci. USA **92:** 2298–2302.

Hayase, A., Takagi, M., Miyazaki, T., Oshiumi, H., Shinohara, M., and Shinohara, A. (2004). A protein complex containing Mei5 and Sae3 promotes the assembly of the meiosis-specific RecA homolog Dmc1. Cell **119:** 927–940.

Higgins, J.D., Armstrong, S.J., Franklin, F.C., and Jones, G.H. (2004). The *Arabidopsis* MutS homolog AtMSH4 functions at an early step in recombination: Evidence for two classes of recombination in *Arabidopsis*. Genes Dev. **18:** 2557–2570.

Hong, E.L., Shinohara, A., and Bishop, D.K. (2001). *Saccharomyces cerevisiae* Dmc1 protein promotes renaturation of single-strand DNA (ssDNA) and assimilation of ssDNA into homologous super-coiled duplex DNA. J. Biol. Chem. **276:** 41906–41912.

Hunter, N., and Kleckner, N. (2001). The single-end invasion: An asymmetric intermediate at the double-strand break to double-holliday junction transition of meiotic recombination. Cell **106:** 59–70.

Kagawa, W., and Kurumizaka, H. (2010). From meiosis to postmeiotic events: Uncovering the molecular roles of the meiosis-specific recombinase Dmc1. FEBS J. **277:** 590–598.

Kagawa, W., Kurumizaka, H., Ikawa, S., Yokoyama, S., and Shibata, T. (2001). Homologous pairing promoted by the human Rad52 protein. J. Biol. Chem. **276:** 35201–35208.

Keeney, S., Giroux, C.N., and Kleckner, N. (1997). Meiosis-specific DNA double-strand breaks are catalyzed by Spo11, a member of a widely conserved protein family. Cell **88:** 375–384.

Keeney, S., and Kleckner, N. (1995). Covalent protein-DNA complexes at the 5′ strand termini of meiosis-specific double-strand breaks in yeast. Proc. Natl. Acad. Sci. USA **92:** 11274–11278.

Kelly, S.M., Jess, T.J., and Price, N.C. (2005). How to study proteins by circular dichroism. Biochim. Biophys. Acta **1751:** 119–139.

Kerzendorfer, C., Vignard, J., Pedrosa-Harand, A., Siwiec, T., Akimcheva, S., Jolivet, S., Sablowski, R., Armstrong, S., Schweizer, D., Mercier, R., and Schlögelhofer, P. (2006). The *Arabidopsis thaliana* MND1 homologue plays a key role in meiotic homologous pairing, synapsis and recombination. J. Cell Sci. **119:** 2486–2496.

Klimyuk, V.I., and Jones, J.D. (1997). AtDMC1, the *Arabidopsis* homologue of the yeast DMC1 gene: Characterization, transposon-induced allelic variation and meiosis-associated expression. Plant J. **11:** 1–14.

Kurzbauer, M.T., Uanschou, C., Chen, D., and Schlögelhofer, P. (2012). The recombinases DMC1 and RAD51 are functionally and spatially separated during meiosis in *Arabidopsis*. Plant Cell **24:** 2058–2070.

Lao, J.P., Oh, S.D., Shinohara, M., Shinohara, A., and Hunter, N. (2008). Rad52 promotes postinvasion steps of meiotic double-strand-break repair. Mol. Cell **29:** 517–524.

Leu, J.Y., Chua, P.R., and Roeder, G.S. (1998). The meiosis-specific Hop2 protein of *S. cerevisiae* ensures synapsis between homologous chromosomes. Cell **94:** 375–386.

Li, W., Chen, C., Markmann-Mulisch, U., Timofejeva, L., Schmelzer, E., Ma, H., and Reiss, B. (2004). The *Arabidopsis* AtRAD51 gene is dispensable for vegetative development but required for meiosis. Proc. Natl. Acad. Sci. USA **101:** 10596–10601.

Li, W., and Ma, H. (2006). Double-stranded DNA breaks and gene functions in recombination and meiosis. Cell Res. **16:** 402–412.

Li, Z., Golub, E.I., Gupta, R., and Radding, C.M. (1997). Recombination activities of HsDmc1 protein, the meiotic human homolog of RecA protein. Proc. Natl. Acad. Sci. USA **94:** 11221–11226.

Malik, S.B., Ramesh, M.A., Hulstrand, A.M., and Logsdon, J.M., Jr.,. (2007). Protist homologs of the meiotic Spo11 gene and topoisomerase VI reveal an evolutionary history of gene duplication and lineage-specific loss. Mol. Biol. Evol. **24:** 2827–2841.

Mancera, E., Bourgon, R., Brozzi, A., Huber, W., and Steinmetz, L.M. (2008). High-resolution mapping of meiotic crossovers and non-crossovers in yeast. Nature **454:** 479–485.

Masson, J.Y., Davies, A.A., Hajibagheri, N., Van Dyck, E., Benson, F.E., Stasiak, A.Z., Stasiak, A., and West, S.C. (1999). The meiosis-specific recombinase hDmc1 forms ring structures and interacts with hRad51. EMBO J. **18:** 6552–6560.

Moffatt, B.A., McWhinnie, E.A., Agarwal, S.K., and Schaff, D.A. (1994). The adenine phosphoribosyltransferase-encoding gene of *Arabidopsis thaliana*. Gene **143:** 211–216.

Masson, J.Y., and West, S.C. (2001). The Rad51 and Dmc1 recombinases: A non-identical twin relationship. Trends Biochem. Sci. **26:** 131–136.

Murayama, Y., Tsutsui, Y., and Iwasaki, H. (2011). The fission yeast meiosis-specific Dmc1 recombinase mediates formation and branch migration of Holliday junctions by preferentially promoting strand exchange in a direction opposite to that of Rad51. Genes Dev. **25:** 516–527.

Muris, D.F., Vreeken, K., Schmidt, H., Ostermann, K., Clever, B., Lohman, P.H., and Pastink, A. (1997). Homologous recombination in the fission yeast *Schizosaccharomyces pombe*: Different requirements for the rhp51+, rhp54+ and rad22+ genes. Curr. Genet. **31:** 248–254.

Neale, M.J., and Keeney, S. (2006). Clarifying the mechanics of DNA strand exchange in meiotic recombination. Nature **442:** 153–158.

Neale, M.J., Pan, J., and Keeney, S. (2005). Endonucleolytic processing of covalent protein-linked DNA double-strand breaks. Nature **436:** 1053–1057.

Niu, H., Wan, L., Baumgartner, B., Schaefer, D., Loidl, J., and Hollingsworth, N.M. (2005). Partner choice during meiosis is regulated by Hop1-promoted dimerization of Mek1. Mol. Biol. Cell **16:** 5804–5818.

Niu, H., et al. (2009). Regulation of meiotic recombination via Mek1-mediated Rad54 phosphorylation. Mol. Cell **36:** 393–404.

Ogawa, T., Yu, X., Shinohara, A., and Egelman, E.H. (1993). Similarity of the yeast RAD51 filament to the bacterial RecA filament. Science **259:** 1896–1899.

Pan, J., Sasaki, M., Kniewel, R., Murakami, H., Blitzblau, H.G., Tischfield, S.E., Zhu, X., Neale, M.J., Jasin, M., Socci, N.D., Hochwagen, A., and Keeney, S. (2011). A hierarchical combination of factors shapes the genome-wide topography of yeast meiotic recombination initiation. Cell **144:** 719–731.

Pâques, F., and Haber, J.E. (1999). Multiple pathways of recombination induced by double-strand breaks in *Saccharomyces cerevisiae*. Microbiol. Mol. Biol. Rev. **63:** 349–404.

Petukhova, G.V., Pezza, R.J., Vanevski, F., Ploquin, M., Masson, J.Y., and Camerini-Otero, R.D. (2005). The Hop2 and Mnd1 proteins act in concert with Rad51 and Dmc1 in meiotic recombination. Nat. Struct. Mol. Biol. **12:** 449–453.

Pezza, R.J., Camerini-Otero, R.D., and Bianco, P.R. (2010). Hop2-Mnd1 condenses DNA to stimulate the synapsis phase of DNA strand exchange. Biophys. J. **99:** 3763–3772.

Pezza, R.J., Petukhova, G.V., Ghirlando, R., and Camerini-Otero, R.D. (2006). Molecular activities of meiosis-specific proteins Hop2, Mnd1, and the Hop2-Mnd1 complex. J. Biol. Chem. **281:** 18426–18434.

Pezza, R.J., Voloshin, O.N., Vanevski, F., and Camerini-Otero, R.D. (2007). Hop2/Mnd1 acts on two critical steps in Dmc1-promoted homologous pairing. Genes Dev. **21:** 1758–1766.

Ploquin, M., Petukhova, G.V., Morneau, D., Déry, U., Bransi, A., Stasiak, A., Camerini-Otero, R.D., and Masson, J.Y. (2007). Stimulation of fission yeast and mouse Hop2-Mnd1 of the Dmc1 and Rad51 recombinases. Nucleic Acids Res. **35:** 2719–2733.

Puizina, J., Siroky, J., Mokros, P., Schweizer, D., and Riha, K. (2004). Mre11 deficiency in *Arabidopsis* is associated with chromosomal instability in somatic cells and Spo11-dependent genome fragmentation during meiosis. Plant Cell **16:** 1968–1978.

Sakane, I., Kamataki, C., Takizawa, Y., Nakashima, M., Toki, S., Ichikawa, H., Ikawa, S., Shibata, T., and Kurumizaka, H. (2008). Filament formation and robust strand exchange activities of the rice DMC1A and DMC1B proteins. Nucleic Acids Res. **36:** 4266–4276.

Sanchez-Moran, E., Santos, J.L., Jones, G.H., and Franklin, F.C. (2007). ASY1 mediates AtDMC1-dependent interhomolog recombination during meiosis in *Arabidopsis*. Genes Dev. **21:** 2220–2233.

Schommer, C., Beven, A., Lawrenson, T., Shaw, P., and Sablowski, R. (2003). AHP2 is required for bivalent formation and for segregation of homologous chromosomes in *Arabidopsis* meiosis. Plant J. **36:** 1–11.

Schwacha, A., and Kleckner, N. (1994). Identification of joint molecules that form frequently between homologs but rarely between sister chromatids during yeast meiosis. Cell **76:** 51–63.

Schwacha, A., and Kleckner, N. (1997). Interhomolog bias during meiotic recombination: Meiotic functions promote a highly differentiated interhomolog-only pathway. Cell **90:** 1123–1135.

Sehorn, M.G., Sigurdsson, S., Bussen, W., Unger, V.M., and Sung, P. (2004). Human meiotic recombinase Dmc1 promotes ATP-dependent homologous DNA strand exchange. Nature **429:** 433–437.

Sheridan, S., and Bishop, D.K. (2006). Red-Hed regulation: recombinase Rad51, though capable of playing the leading role, may be relegated to supporting Dmc1 in budding yeast meiosis. Genes Dev. **20:** 1685–1691.

Sheridan, S.D., Yu, X., Roth, R., Heuser, J.E., Sehorn, M.G., Sung, P., Egelman, E.H., and Bishop, D.K. (2008). A comparative analysis of Dmc1 and Rad51 nucleoprotein filaments. Nucleic Acids Res. **36:** 4057–4066.

Shinohara, A., Gasior, S., Ogawa, T., Kleckner, N., and Bishop, D.K. (1997). *Saccharomyces cerevisiae* recA homologues RAD51 and DMC1 have both distinct and overlapping roles in meiotic recombination. Genes Cells **2:** 615–629.

Shinohara, A., Ogawa, H., and Ogawa, T. (1992). Rad51 protein involved in repair and recombination in *S. cerevisiae* is a RecA-like protein. Cell **69:** 457–470.

Siaud, N., Dray, E., Gy, I., Gérard, E., Takvorian, N., and Doutriaux, M.P. (2004). Brca2 is involved in meiosis in *Arabidopsis thaliana* as suggested by its interaction with Dmc1. EMBO J. **23:** 1392–1401.

Stronghill, P., Pathan, N., Ha, H., Supijono, E., and Hasenkampf, C. (2010). Ahp2 (Hop2) function in *Arabidopsis thaliana* (Ler) is required for stabilization of close alignment and synaptonemal complex formation except for the two short arms that contain nucleolus organizer regions. Chromosoma **119:** 443–458.

Studier, F.W. (2005). Protein production by auto-induction in high density shaking cultures. Protein Expr. Purif. **41:** 207–234.

Sung, P. (1994). Catalysis of ATP-dependent homologous DNA pairing and strand exchange by yeast RAD51 protein. Science **265:** 1241–1243.

Tashiro, S., Kotomura, N., Shinohara, A., Tanaka, K., Ueda, K., and Kamada, N. (1996). S phase specific formation of the human Rad51 protein nuclear foci in lymphocytes. Oncogene **12:** 2165–2170.

Tashiro, S., Walter, J., Shinohara, A., Kamada, N., and Cremer, T. (2000). Rad51 accumulation at sites of DNA damage and in postreplicative chromatin. J. Cell Biol. **150:** 283–291.

Tsubouchi, H., and Roeder, G.S. (2002). The Mnd1 protein forms a complex with hop2 to promote homologous chromosome pairing and meiotic double-strand break repair. Mol. Cell. Biol. **22:** 3078–3088.

Tsubouchi, H., and Roeder, G.S. (2006). Budding yeast Hed1 down-regulates the mitotic recombination machinery when meiotic recombination is impaired. Genes Dev. **20:** 1766–1775.

Vignard, J., Siwiec, T., Chelysheva, L., Vrielynck, N., Gonord, F., Armstrong, S.J., Schlögelhofer, P., and Mercier, R. (2007). The interplay of RecA-related proteins and the MND1-HOP2 complex during meiosis in *Arabidopsis thaliana*. PLoS Genet. **3:** 1894–1906.

Wan, L., de los Santos, T., Zhang, C., Shokat, K., and Hollingsworth, N.M. (2004). Mek1 kinase activity functions downstream of RED1 in the regulation of meiotic double strand break repair in budding yeast. Mol. Biol. Cell **15:** 11–23.

Wijnker, E., van Dun, K., de Snoo, C.B., Lelivelt, C.L., Keurentjes, J.J., Naharudin, N.S., Ravi, M., Chan, S.W., de Jong, H., and Dirks, R. (2012). Reverse breeding in *Arabidopsis thaliana* generates homozygous parental lines from a heterozygous plant. Nat. Genet. **44:** 467–470.

Yamamoto, A., Taki, T., Yagi, H., Habu, T., Yoshida, K., Yoshimura, Y., Yamamoto, K., Matsushiro, A., Nishimune, Y., and Morita, T. (1996). Cell cycle-dependent expression of the mouse Rad51 gene in proliferating cells. Mol. Gen. Genet. **251:** 1–12.

Yu, X., and Egelman, E.H. (2010). Helical filaments of human Dmc1 protein on single-stranded DNA: A cautionary tale. J. Mol. Biol. **401:** 544–551.

Zenvirth, D., Loidl, J., Klein, S., Arbel, A., Shemesh, R., and Simchen, G. (1997). Switching yeast from meiosis to mitosis: Double-strand break repair, recombination and synaptonemal complex. Genes Cells **2:** 487–498.

Zhao, W., et al. (October 22, 2013). Mechanistic insights into the role of Hop2-Mnd1 in meiotic homologous DNA pairing. Nucleic Acids Res. doi/10.1093/nar/gkt924.

Zierhut, C., Berlinger, M., Rupp, C., Shinohara, A., and Klein, F. (2004). Mnd1 is required for meiotic interhomolog repair. Curr. Biol. **14:** 752–762.